Serious Numerics for Serious Physics: Nonlocal Transport Hydrodynamic Model on Curvilinear Meshes

Milan Holec

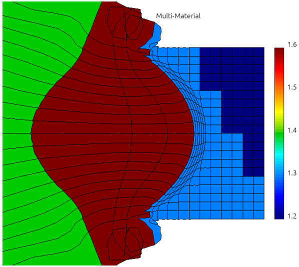

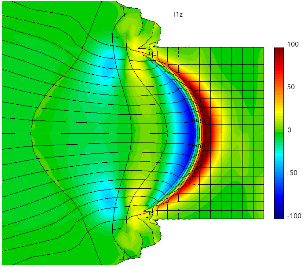

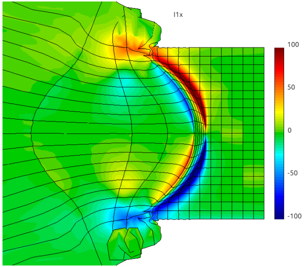

CASC, LLNL
Livermore, CA, USA
January 16, 2018

1. Introduction to Nonlocal Transport Hydrodynamic model (NTH)
   - Thermal radiative transfer
   - Nonlocal electron transport
2. High-order discontinuous Galerkin BGK transport scheme for hydrodynamics (DG-BGK&T)
   - DG-BGK&T finite element transport scheme
   - Nonlocal transport on curvilinear meshes
   - DG-BGK&T + LAGHOS
3. Application of NTH in high-power laser physics
   - Nonlocal transport hydrodynamic model for laser-heated plasmas
   - Measurement of preheat due to nonlocal electron transport in warm dense matter
   - The effect of pre-plasma formation under nonlocal transport conditions for ultra-relativistic laser-plasma interaction
4. Extras...
5. Conclusions

Thermal Radiative Transfer

Radiation transport equation

The radiation intensity $I_\nu(\boldsymbol{x}, \boldsymbol{n})$ representing photons of frequency ν obeys the equation

$$\boldsymbol{n} \cdot \nabla I_\nu = \eta_\nu - \chi_\nu I_\nu,$$

where *emmisivity* $\eta_\nu(\rho, T)$ and absorptivity $\chi_\nu(\rho, T)$ are considered to be isotropic.

$$\begin{aligned} \nabla \cdot \boldsymbol{q}_\nu &= 4\pi\eta_\nu - \chi_\nu E_\nu \\ \nabla \cdot \mathbf{P}_\nu &= -\frac{\chi_\nu}{c}\boldsymbol{q}_\nu \end{aligned}$$

Radiation diffusion

In the case of low anisotropy pressure tensor can be approximated as $\mathbf{P}_\nu = \mathbf{I} f_\nu E_\nu$ and the radiation field can be modeled by

$$\nabla \cdot \left(\frac{c}{\chi_\nu} \nabla (f_\nu E_\nu) \right) = \chi_\nu E_\nu - 4\pi\eta_\nu,$$

where the lowest anisotropy approximation $\tilde{I}_\nu(\boldsymbol{x}, \boldsymbol{n}) = I^0_\nu(\boldsymbol{x}) + \boldsymbol{n} \cdot \boldsymbol{I}^1_\nu(\boldsymbol{x})$ corresponds to the *variable Eddington factor* $f_\nu = \frac{1}{3}$.

[1]

[1] D. Mihalas and B. Mihalas, Foundations of Radiation Hydrodynamics (Oxford University Press, New York, 1985).

Radiation-Hydrodynamic model of plasma

Boltzmann transport equation

$$\frac{\partial f}{\partial t} + \boldsymbol{v} \cdot \nabla_x f + \frac{q_e}{m_e}\left(\boldsymbol{E} + \frac{\boldsymbol{v}}{c} \times \boldsymbol{B}\right) \cdot \nabla_{\boldsymbol{v}} f = \sigma \nabla_{\boldsymbol{v}} \cdot \int \frac{|\boldsymbol{v} - \boldsymbol{v}'|^2 \mathbf{I} - (\boldsymbol{v} - \boldsymbol{v}') \otimes \boldsymbol{v} - \boldsymbol{v}')}{|\boldsymbol{v} - \boldsymbol{v}'|^3} (\nabla_{\boldsymbol{v}} f(\boldsymbol{v}) f(\boldsymbol{v}') - f(\boldsymbol{v}) \nabla_{\boldsymbol{v}} f(\boldsymbol{v}')) \mathrm{d}\boldsymbol{v}'$$

Fluid equations

$$\begin{aligned}
\frac{\mathrm{d}\rho}{\mathrm{d}t} &= -\rho \nabla_{\boldsymbol{x}} \cdot \boldsymbol{U} \\
\rho \frac{\mathrm{d}\boldsymbol{U}}{\mathrm{d}t} &= \nabla_{\boldsymbol{x}} \cdot \sigma \\
\rho \frac{\mathrm{d}\varepsilon}{\mathrm{d}t} &= \sigma : \nabla_{\boldsymbol{x}} \boldsymbol{U} - \nabla_{\boldsymbol{x}} \cdot (\boldsymbol{q}_e + \boldsymbol{q}_R)
\end{aligned}$$

Microscopic closure

$$\begin{aligned}
\sigma &= -\rho \int (\boldsymbol{v} - \boldsymbol{U}) \otimes (\boldsymbol{v} - \boldsymbol{U})\, f \,\mathrm{d}\boldsymbol{v}^3 \approx -\mathbf{I}p + \tilde{\sigma}(\nabla \boldsymbol{U}) \\
\boldsymbol{q}_e &= \frac{\rho}{2} \int |\boldsymbol{v} - \boldsymbol{U}|^2 (\boldsymbol{v} - \boldsymbol{U})\, f \,\mathrm{d}\boldsymbol{v}^3 \approx \frac{\rho}{2} \int_{4\pi} \boldsymbol{n} \int_0^\infty |\boldsymbol{v}|^5 f \,\mathrm{d}|\boldsymbol{v}| \,\mathrm{d}\boldsymbol{n} \approx -\kappa(T^{2.5}) \nabla T \\
\boldsymbol{q}_R &= \int_{4\pi} \boldsymbol{n} \int_\nu I_\nu^p \,\mathrm{d}\nu \,\mathrm{d}\boldsymbol{n} \approx -\int_\nu \frac{c}{\chi_\nu} \nabla (f_\nu E_\nu) \,\mathrm{d}\nu
\end{aligned}$$

BGK collision operator

$$C_{ei}(f^e, f^i) \overset{m_e/m_i}{\approx} \sigma \nabla_v \cdot \left(\frac{1}{v} \left(\mathbf{I} - \frac{\mathbf{v} \otimes \mathbf{v}}{v^2} \right) \cdot \nabla_v f^e \right)$$

$$\overset{\text{spher}}{\approx} \frac{\sigma}{v^3} \frac{1}{\sin(\phi)} \left[\frac{\partial}{\partial \phi} \left(\sin(\phi) \frac{\partial f^e}{\partial \phi} \right) + \frac{1}{\sin(\phi)} \frac{\partial^2 f^e}{\partial \theta^2} \right]$$

$$\overset{f^0+f^1\cos(\phi)}{\approx} -\frac{2\sigma}{v^3} f_1^e \cos(\phi) = 2\nu_{ei} \left(f_0^e - f^e \right)$$

Then, the electron distribution function can be governed by the BGK Boltzmann transport equation

$$\boldsymbol{n} \cdot \nabla_x f^e + \frac{q_e}{m_e |\boldsymbol{v}|} \boldsymbol{E} \cdot \nabla_{\boldsymbol{v}} f^e = \frac{2(f_{MB}(|\boldsymbol{v}|, T_e) - f^e)}{\lambda_{ei}},$$

where f_{MB} is the Maxwell-Boltzmann equilibrium distribution and λ_{ei} the electron mean free path when scattered on ions.

Chapman-Enskog approximation in small parameter λ_{ei}

$$f^e = f_0 + \lambda_{ei} f_1 + O(\lambda_{ei}{}^2) \approx f_{MB}(|\boldsymbol{v}|, T_e) - f_{MB}(|\boldsymbol{v}|, T_e) g(\bar{Z}) \left(\frac{|\boldsymbol{v}|^2}{2 v_{T_e}^2} - 4 \right) \boldsymbol{n} \cdot \frac{\lambda_{ei} \nabla T_e}{T_e}$$

$$\rightarrow \boldsymbol{q}_{SH} = \kappa_{SH} T_e^{\frac{5}{2}} \nabla T_e$$

$$\frac{\lambda_{ei} f_1}{f_0} = 0.25 \left(\frac{|\boldsymbol{v}|^2}{2 v_{T_e}^2} - 4 \right) \boldsymbol{n} \cdot \frac{\lambda_{ei} (|\boldsymbol{v}|^4) \nabla T_e}{T_e} < 0.1 \quad \longrightarrow \quad \mathrm{Kn}^e = \frac{\lambda_{ei} \nabla T_e}{T_e} < 7.5 \times 10^{-4}$$

Nonlocal Transport Hydrodynamic model

$$
\begin{aligned}
\frac{\mathrm{d}\rho}{\mathrm{d}t} &= -\rho\nabla\cdot\boldsymbol{u}\,,\\
\rho\frac{\mathrm{d}\boldsymbol{u}}{\mathrm{d}t} &= -\nabla(p_i+p_e)\,,\\
\rho\left(\frac{\partial\varepsilon_i}{\partial T_i}\frac{\mathrm{d}T_i}{\mathrm{d}t}+\frac{\partial\varepsilon_i}{\partial\rho}\frac{\mathrm{d}\rho}{\mathrm{d}t}\right) &= -p_i\nabla\cdot\boldsymbol{u}-G(T_i-T_e)\,,\\
\rho\left(\frac{\partial\varepsilon_e}{\partial T_e}\frac{\mathrm{d}T_e}{\mathrm{d}t}+\frac{\partial\varepsilon_e}{\partial\rho}\frac{\mathrm{d}\rho}{\mathrm{d}t}\right) &= -p_e\nabla\cdot\boldsymbol{u}-\nabla\cdot(\boldsymbol{q}_e+\boldsymbol{q}_R)+G(T_i-T_e)+Q_{\mathrm{IB}}(\boldsymbol{E}_L)\,,
\end{aligned}
$$

the quantities $\frac{\partial\varepsilon}{\partial\rho}=\frac{\partial f}{\partial\rho}-T\frac{\partial^2 f}{\partial\rho\partial T}$, $\frac{\partial\varepsilon}{\partial T}=-T\frac{\partial^2 f}{\partial T^2}$, $p=\rho^2\frac{\partial f}{\partial\rho}$, $G=\rho\frac{\partial\varepsilon_e}{\partial T_e}\nu_{ei}$ provides our HerEOS equation of state.

Nonlocal transport of photon intensity
$I^p=\int_\nu f^p\frac{h^4\nu^3}{c^2}\,\mathrm{d}\nu$

$$\boldsymbol{n}\cdot\nabla I^p=\frac{aT_e^4-I^p}{\lambda^p}$$

Radiation closure relations

$$\boldsymbol{q}_R=\int_{4\pi}\boldsymbol{n}\,I^p\,\mathrm{d}\boldsymbol{n}\xrightarrow{\text{diffusive}}\nabla\cdot\boldsymbol{q}_R=-\nabla\cdot\left(\frac{c}{3\chi_R}\nabla E\right)$$

Nonlocal transport of electron intensity $I^e=\int_\nu f^e\frac{m_e|\boldsymbol{v}|^5}{2}\,\mathrm{d}|\boldsymbol{v}|$

$$\boldsymbol{n}\cdot\nabla I^e=k_B\left(n_i\frac{\mathrm{d}\bar{Z}}{\mathrm{d}t}\frac{3}{8\pi}+\frac{n_e\sqrt{2}}{8.51\lambda^{ei}\pi^{\frac{3}{2}}}v_{T_e}\right)T_e-\frac{I^e}{8.51\lambda^{ei}}$$

Electron closure relations

$$\boldsymbol{q}_e=\int_{4\pi}\boldsymbol{n}\,I^e\,\mathrm{d}\boldsymbol{n}\xrightarrow{\text{diffusive}}\nabla\cdot\boldsymbol{q}_e=-\nabla\cdot\left(\kappa_{SH}\,T_e^{\frac{5}{2}}\,\nabla T_e\right)$$

Planar geometry - transport equation

$$\cos(\Phi)\frac{\partial I}{\partial z} = S_T T_e - kI \,,$$

$$I(t,z,\Phi) = (\boldsymbol{\omega}_\Phi \otimes \boldsymbol{\psi}_z)^T \cdot \boldsymbol{I}^{n+1},\ T_e(t,z) = \boldsymbol{\phi}_z^T \cdot \boldsymbol{T}_e^{n+1}$$

Composition of the multi-dimensional interpolation based on *outerproduct*$\otimes$

$$\boldsymbol{\omega}_\Phi = [\omega_1(\Phi),..,\omega_{M_\Phi}(\Phi)]^T, \boldsymbol{\psi}_z = [\psi_1(z),..,\psi_{N_f}(z)]^T,\ \boldsymbol{\phi}_z = [\phi_1(z),..,\phi_{N_e}(z)]^T$$

$$\int_{\Omega_\Phi}\int_{\Omega_z} (\boldsymbol{\omega}_\Phi \otimes \boldsymbol{\psi}_z) \otimes \left[\cos(\Phi)\left(\boldsymbol{\omega}_\Phi \otimes \frac{\partial \boldsymbol{\psi}_z}{\partial z}\right)^T \cdot \boldsymbol{I}^{n+1} + k\,(\boldsymbol{\omega}_\Phi \otimes \boldsymbol{\psi}_z)^T \cdot \boldsymbol{I}^{n+1} - (\boldsymbol{\omega}_\Phi \otimes \boldsymbol{\phi}_z)^T \cdot \mathbf{S}_T \cdot \boldsymbol{T_e}^{n+1}\right] \mathrm{d}\Omega_z \,\sin(\Phi)\,\mathrm{d}\Phi =$$

$$\int_{\Omega_\Phi}\int_{\Gamma_{\boldsymbol{n}\cdot\boldsymbol{n}_\Gamma<0}} (\boldsymbol{\omega}_\Phi \otimes \boldsymbol{\psi}_z) \otimes \left[(\boldsymbol{\omega}_\Phi \otimes \boldsymbol{\psi}_z)^T \cdot \boldsymbol{I}^{n+1} - \left(\boldsymbol{\omega}_\Phi \otimes \tilde{\boldsymbol{\psi}}_z\right)^T \cdot \tilde{\boldsymbol{I}}\right] (\cos(\Phi)\boldsymbol{n}_\Gamma^z)\ \mathrm{d}\Gamma_z \,\sin(\Phi)\,\mathrm{d}\Phi$$

Discrete DG transport equation - transport operator inversion $\boldsymbol{I}^{n+1} = \mathbf{A} \cdot \boldsymbol{T}_e^{n+1} + \boldsymbol{b}(\tilde{\boldsymbol{I}})$

$$\mathbf{D} \cdot \boldsymbol{I}^{n+1} + k\mathbf{M} \cdot \boldsymbol{I}^{n+1} - \mathbf{B} \cdot \boldsymbol{I}^{n+1} = \mathbf{S} \cdot \boldsymbol{T_e}^{n+1} - \tilde{\mathbf{B}} \cdot \tilde{\boldsymbol{I}}$$

[2]

[2] M. Holec, J. Limpouch, R. Liska and S. Weber, *Int. J. Numer. Meth. F.*, 83, 779 (2017).

Exact steady state "given direction" transport

$$\cos(\Phi_0)\,\frac{\mathrm{d}I(z,\Phi_0)}{\mathrm{d}z} = k\,(\sin(\pi z) - I(z,\Phi_0))$$

Three different values of $k = 10^{-4}, 1, 10^{4}$, which corresponds to free-streaming, nonlocal, and diffusive transport ($\Phi_0 = \pi/4$).

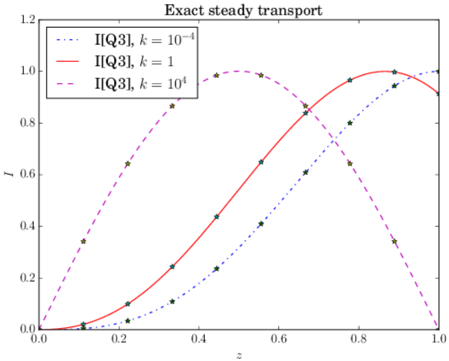

element	cells	$E_{L1}^{k=10^{-4}}$	$q_{L1}^{k=10^{-4}}$	$E_{L1}^{k=1}$	$q_{L1}^{k=1}$	$E_{L1}^{k=10^{4}}$	$q_{L1}^{k=10^{4}}$
I[Q1]	10	2.7e-07		2.3e-03		8.3e-03	
I[Q1]	20	4.9e-08	2.5	4.3e-04	2.4	1.6e-03	2.4
I[Q1]	40	1.2e-08	2.0	1.1e-04	2.0	3.7e-04	2.1
I[Q1]	80	2.9e-09	2.0	2.6e-05	2.0	9.0e-05	2.1
I[Q2]	10	4.6e-09		4.1e-05		3.5e-07	
I[Q2]	20	4.1e-10	3.5	3.5e-06	3.5	5.2e-08	2.8
I[Q2]	40	4.5e-11	3.2	4.0e-07	3.2	1.2e-08	2.1
I[Q2]	80	5.4e-12	3.1	4.7e-08	3.1	2.8e-09	2.1
I[Q3]	10	7.3e-11		2.6e-07		2.3e-06	
I[Q3]	20	2.8e-12	4.7	8.4e-09	5.0	1.0e-07	4.5
I[Q3]	40	1.5e-13	4.2	4.3e-10	4.3	5.6e-09	4.2
I[Q3]	80	8.9e-15	4.1	2.4e-11	4.1	3.3e-10	4.1

It is worth mentioning that the method works well also in diffusive limit $k = 10^{4}$ ($Kn \approx 10^{-4}$).

[2] M. Holec, J. Limpouch, R. Liska and S. Weber, *Int. J. Numer. Meth. F.*, 83, 779 (2017).

Exact steady state "full" transport

Model steady equation

$$\cos(\Phi)\,\frac{\mathrm{d}I(z,\Phi)}{\mathrm{d}z} = k\,(S(z) - I(z,\Phi))$$

Energy density flux

$$\boldsymbol{q}(z) = 2\pi\int_0^\pi \cos(\Phi)\, I(z,\Phi)\, \sin(\Phi)\,\mathrm{d}\Phi$$

Divergence of energy density flux

$$\nabla\cdot\boldsymbol{q}(z) = 2\pi\int_0^\pi \cos(\Phi)\,\frac{\partial I(z,\Phi)}{\partial z}\,\sin(\Phi)\,\mathrm{d}\Phi$$

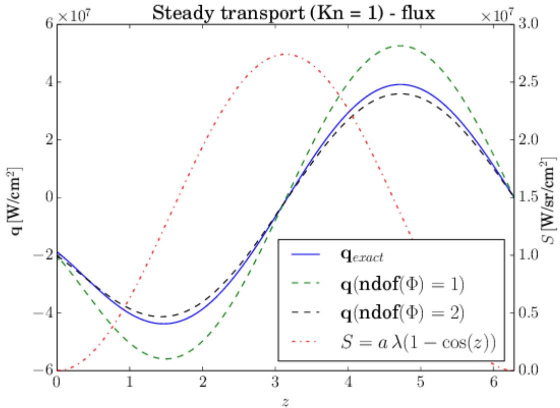

Relative L1 error convergence in polar angle Φ of $\nabla\cdot\boldsymbol{q}$

transport regime	Kn=λ/L — ndof(Φ)	1	2	3	4	5	20	40
transparent/ballistic	100.0	1.5e-01	4.1e-01	9.5e-02	2.4e-01	7.1e-02	5.1e-02	2.2e-02
nonlocal/highly anisotropic	10.0	2.0e-01	3.7e-01	1.1e-01	2.0e-01	7.8e-02	1.3e-02	1.1e-03
nonlocal/anisotropic	1.0	3.5e-01	8.8e-02	2.6e-02	1.1e-02	2.7e-03	1.1e-05	9.6e-07
nonlocal/almost isotropic	0.1	1.5e-01	9.6e-03	4.8e-03	3.3e-3	6.9e-04	5.7e-07	4.6e-07
diffusive/isotropic	0.01	1.4e-01	1.0e-02	5.9e-03	4.5e-03	2.0e-03	2.9e-05	2.9e-05

[2] M. Holec, J. Limpouch, R. Liska and S. Weber, *Int. J. Numer. Meth. F.*, 83, 779 (2017).

Planar geometry - transport equation

$$\cos(\Phi)\frac{\partial I}{\partial z} = S_T T_e - (k + \sigma + \cos(\Phi) E_z) I + \sigma I_0\,, \quad I_0 = \frac{1}{2}\int_{\Omega_\Phi} I \sin(\Phi)\, \mathrm{d}\Phi$$

$$I(t, z, \Phi) = (\boldsymbol{\omega}_\Phi \otimes \boldsymbol{\psi}_z)^T \cdot \boldsymbol{I}^{n+1},\ T_e(t, z) = \boldsymbol{\phi}_z^T \cdot \boldsymbol{T}_e^{n+1}$$

Composition of the multi-dimensional interpolation based on *outerproduct* $\otimes$

$$\boldsymbol{\omega}_\Phi = [\omega_1(\Phi), .., \omega_{M_\Phi}(\Phi)]^T, \boldsymbol{\psi}_z = [\psi_1(z), .., \psi_{N_f}(z)]^T,\ \boldsymbol{\phi}_z = [\phi_1(z), .., \phi_{N_e}(z)]^T$$

$$\int_{\Omega_\Phi}\int_{\Omega_z} (\boldsymbol{\omega}_\Phi \otimes \boldsymbol{\psi}_z) \otimes \Bigg[\cos(\Phi)\left(\boldsymbol{\omega}_\Phi \otimes \frac{\partial \boldsymbol{\psi}_z}{\partial z}\right)^T \cdot \boldsymbol{I}^{n+1} + (k + \cos(\Phi) E_z)\,(\boldsymbol{\omega}_\Phi \otimes \boldsymbol{\psi}_z)^T \cdot \boldsymbol{I}^{n+1} - \frac{\sigma}{2}\int_{\Omega_\Phi} \boldsymbol{\omega}_\Phi^T \sin(\Phi) \mathrm{d}\Phi \otimes \boldsymbol{\psi}_z^T \cdot \boldsymbol{I}^{n+1}$$

$$- (\boldsymbol{\omega}_\Phi \otimes \boldsymbol{\phi}_z)^T \cdot \mathbf{S}_T \cdot \boldsymbol{T_e}^{n+1}\Bigg] \mathrm{d}\Omega_z \sin(\Phi)\, \mathrm{d}\Phi =$$

$$\int_{\Omega_\Phi}\int_{\Gamma_{\boldsymbol{n}\cdot\boldsymbol{n}_\Gamma < 0}} (\boldsymbol{\omega}_\Phi \otimes \boldsymbol{\psi}_z) \otimes \left[(\boldsymbol{\omega}_\Phi \otimes \boldsymbol{\psi}_z)^T \cdot \boldsymbol{I}^{n+1} - \left(\boldsymbol{\omega}_\Phi \otimes \tilde{\boldsymbol{\psi}}_z\right)^T \cdot \tilde{\boldsymbol{I}}\right] (\cos(\Phi) \boldsymbol{n}_\Gamma^z)\ \mathrm{d}\Gamma_z \sin(\Phi)\, \mathrm{d}\Phi$$

Discrete DG transport equation - transport operator inversion $\quad \boldsymbol{I}^{n+1} = \mathbf{A} \cdot \boldsymbol{T}_e^{n+1} + \boldsymbol{b}(\tilde{\boldsymbol{I}})$

$$\mathbf{D} \cdot \boldsymbol{I}^{n+1} + ((k + \sigma)\mathbf{M} + E_z \mathbf{M}_{\cos(\Phi)} - \sigma \mathbf{MI}) \cdot \boldsymbol{I}^{n+1} - \mathbf{B} \cdot \boldsymbol{I}^{n+1} = \mathbf{S} \cdot \boldsymbol{T_e}^{n+1} - \tilde{\mathbf{B}} \cdot \tilde{\boldsymbol{I}}$$

[2] M. Holec, J. Limpouch, R. Liska and S. Weber, *Int. J. Numer. Meth. F.*, 83, 779 (2017).

Planar geometry - energy equation equipped with the nonlocal transport

$$a\frac{\mathrm{d}T_e}{\mathrm{d}t} + G_{ei}(T_e - T_i) + \int_{4\pi} \cos(\Phi)\frac{\partial I}{\partial z}\sin(\Phi)\,\mathrm{d}\Phi\,\mathrm{d}\Theta = P_e$$

$$I(t,z,\Phi) = (\boldsymbol{\omega}_\Phi \otimes \boldsymbol{\psi}_z)^T \cdot \boldsymbol{I}^{n+1},\ T_e(t,z) = \boldsymbol{\phi}_z^T \cdot \boldsymbol{T}_e^{n+1},\ T_i(t,z) = \tilde{\boldsymbol{\phi}}_z{}^T \cdot \boldsymbol{T}_i^{n+1}$$

$$\int_{\Omega_z} \boldsymbol{\phi}_z \otimes \Bigg[a\,\boldsymbol{\phi}_z^T \cdot \frac{\boldsymbol{T}_e^{n+1} - \boldsymbol{T}_e^n}{\Delta t} + G_{ei}\left(\boldsymbol{\phi}_z^T \cdot \boldsymbol{T}_e^{n+1} - \tilde{\boldsymbol{\phi}}_z{}^T \cdot \boldsymbol{T}_i^{n+1}\right) + 2\pi \int_{\Omega_\Phi} \cos(\Phi)\left(\boldsymbol{\omega}_\Phi \otimes \frac{\partial \boldsymbol{\psi}_z}{\partial z}\right)^T \cdot \boldsymbol{I}^{n+1}\sin(\Phi)\,\mathrm{d}\Phi - \boldsymbol{\phi}_z^T \cdot \boldsymbol{P}_e\Bigg]\mathrm{d}\Omega_z = \mathbf{0}\,.$$

$$a\mathbf{M} \cdot \frac{\boldsymbol{T}_e^{n+1} - \boldsymbol{T}_e^n}{\Delta t} + \mathbf{G}_{ei} \cdot \boldsymbol{T}_e^{n+1} - \tilde{\mathbf{G}}_{ei} \cdot \boldsymbol{T}_i^{n+1} + \mathbf{DI} \cdot \boldsymbol{I}^{n+1} = \boldsymbol{P}_e$$

DG-BGK&Ts scheme, where $\boldsymbol{I}^{n+1} = \mathbf{A} \cdot \boldsymbol{T}_e^{n+1} + \boldsymbol{b}$

$$\mathbf{A}_{T_e}(\mathbf{A}) \cdot \boldsymbol{T}_e^{n+1} + \tilde{\mathbf{G}}_{ei} \cdot \boldsymbol{T}_i^{n+1} = \boldsymbol{b}_{T_e}(\boldsymbol{b})$$

M. Holec, J. Limpouch, R. Liska and S. Weber, *Int. J. Numer. Meth. F.*, 83, 779 (2017).

Approximate multi-group diffusion test

Two energy groups transport model

$$\cos(\Phi)\,\frac{\partial I_{g_j}}{\partial z} = k_{g_j}\left(S_T T - I_{g_j}\right)$$

$$a\,\frac{\partial T}{\partial t} = -\sum_{j=1,2}\frac{2\pi}{\Delta_{g_j}}\int_0^{\pi}\cos(\Phi)\,\frac{\partial I_{g_j}}{\partial z}\,\sin(\Phi)\,d\Phi\ ,$$

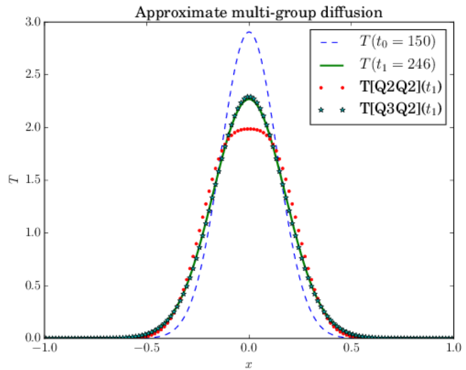

Diffusive(local) asymptotic behavior of the two energy groups transport model

$$I_{g_j} \approx S_T\left(T - \frac{\cos(\Phi)}{k_{g_j}}\frac{\partial T}{\partial z}\right) \xrightarrow{local} a\frac{\partial T}{\partial t} \approx \frac{4\pi S_T}{3}\left(\frac{1}{k_{g_1}\Delta_{g_1}} + \frac{1}{k_{g_2}\Delta_{g_2}}\right)\frac{\partial^2 T}{\partial z^2}\ .$$

cells	32	64	128	256	512
T[Q1Q1]	2.2e-01 [5]	2.4e-01 (-0.1)	2.3e-01 (0.0)	2.3e-01 (0.0)	2.3e-01 (0.0)
T[Q2Q2]	8.7e-02 [4]	9.5e-02 (-0.1)	9.8e-02 (-0.0)	9.6e-02 (0.0)	9.1e-02 (0.1)
T[Q3Q2]	1.2e-01 [4]	5.7e-02 (1.1)	1.0e-02 (2.5)	1.3e-03 (2.9)	–
T[Q3Q3]	7.6e-02 [4]	4.6e-02 (0.7)	9.8e-03 (2.2)	1.3e-03 (2.9)	–
T[Q4Q4]	2.9e-02 [4]	9.6e-03 (1.6)	1.3e-03 (2.9)	–	–
T[Q5Q5]	2.3e-03 [4]	8.2e-05 (4.8)	–	–	–
T[Q6Q6]	1.7e-04 [4]	–	–	–	–

[2] M. Holec, J. Limpouch, R. Liska and S. Weber, *Int. J. Numer. Meth. F.*, 83, 779 (2017).

Lagrangian High-Order Curvilinear Framework

$$
\begin{aligned}
\mathbf{M}_{\boldsymbol{v}} \cdot \frac{\mathrm{d}\boldsymbol{v}}{\mathrm{d}t} &= -\mathbf{F} \cdot \mathbf{I} \\
\mathbf{M}_{e} \cdot \frac{\mathrm{d}\boldsymbol{e}}{\mathrm{d}t} &= \mathbf{F}^{T} \cdot \boldsymbol{v} \\
\frac{\mathrm{d}\boldsymbol{x}}{\mathrm{d}t} &= \boldsymbol{v}
\end{aligned}
$$

[Dobrev, Kolev, Rieben, SIAM JSC 34, B606 (2012)]

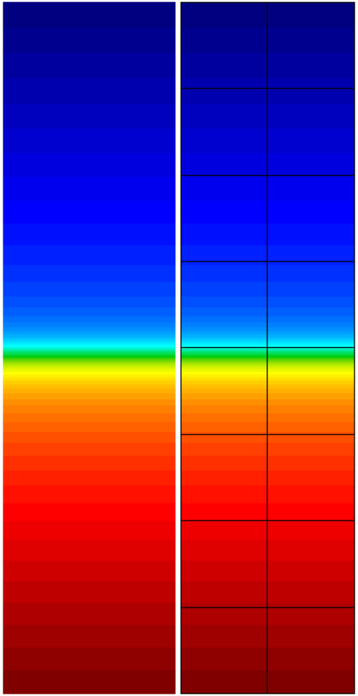

Lagrangian High-Order Curvilinear Framework

$$
\begin{aligned}
\mathbf{M}_{\boldsymbol{v}} \cdot \frac{\mathrm{d}\boldsymbol{v}}{\mathrm{d}t} &= -\mathbf{F} \cdot \mathbf{I} \\
\mathbf{M}_{e} \cdot \frac{\mathrm{d}\boldsymbol{e}}{\mathrm{d}t} &= \mathbf{F}^{T} \cdot \boldsymbol{v} \\
\frac{\mathrm{d}\boldsymbol{x}}{\mathrm{d}t} &= \boldsymbol{v}
\end{aligned}
$$

[Dobrev, Kolev, Rieben, SIAM JSC 34, B606 (2012)]

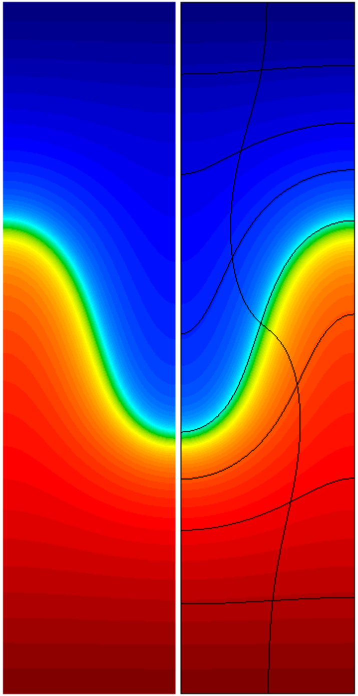

Lagrangian High-Order Curvilinear Framework

$$
\begin{aligned}
\mathbf{M}_{\boldsymbol{v}} \cdot \frac{\mathrm{d}\boldsymbol{v}}{\mathrm{d}t} &= -\mathbf{F} \cdot \mathbf{I} \\
\mathbf{M}_{e} \cdot \frac{\mathrm{d}\boldsymbol{e}}{\mathrm{d}t} &= \mathbf{F}^{T} \cdot \boldsymbol{v} \\
\frac{\mathrm{d}\boldsymbol{x}}{\mathrm{d}t} &= \boldsymbol{v}
\end{aligned}
$$

[Dobrev, Kolev, Rieben, SIAM JSC 34, B606 (2012)]

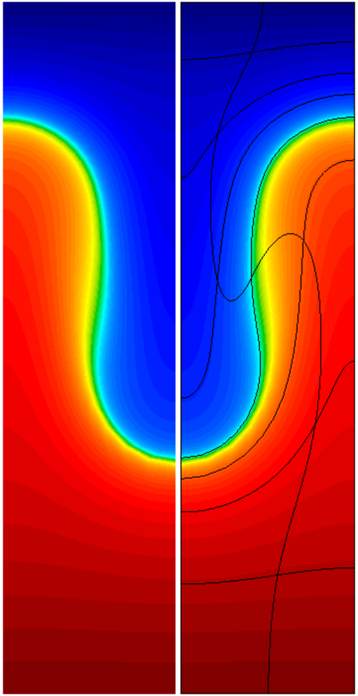

Lagrangian High-Order Curvilinear Framework

$$
\begin{aligned}
\mathbf{M}_{\boldsymbol{v}} \cdot \frac{d\boldsymbol{v}}{dt} &= -\mathbf{F} \cdot \mathbf{1} \\
\mathbf{M}_{e} \cdot \frac{d\boldsymbol{e}}{dt} &= \mathbf{F}^{T} \cdot \boldsymbol{v} \\
\frac{d\boldsymbol{x}}{dt} &= \boldsymbol{v}
\end{aligned}
$$

[Dobrev, Kolev, Rieben, SIAM JSC 34, B606 (2012)]

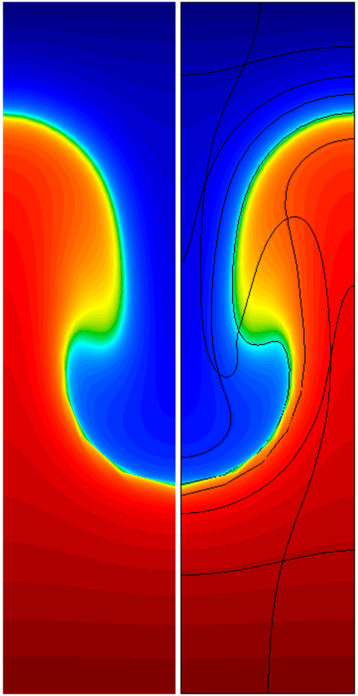

Nonlocal Extension of Lagrangian High-Order Curvilinear Framework

$$
\begin{aligned}
\mathbf{M}_{\boldsymbol{v}} \cdot \frac{\mathrm{d}\boldsymbol{v}}{\mathrm{d}t} &= -\mathbf{F} \cdot \mathbf{I} \\
k_B \mathbf{M}_e \cdot \frac{\mathrm{d}\boldsymbol{T}}{\mathrm{d}t} &= \mathbf{F}^T \cdot \boldsymbol{v} - \int_{4\pi} \mathbf{D} \cdot \boldsymbol{I} \,\mathrm{d}\boldsymbol{n} \\
\frac{\mathrm{d}\boldsymbol{x}}{\mathrm{d}t} &= \boldsymbol{v} \\
\mathbf{D} \cdot \boldsymbol{I} &= \mathbf{S} \cdot \boldsymbol{T} - ((k + \sigma)\mathbf{M} + \boldsymbol{E} \cdot \mathbf{M}_{\boldsymbol{n}} - \sigma \mathbf{MI}) \cdot \boldsymbol{I} + \mathbf{B} \cdot \boldsymbol{I} - \tilde{\mathbf{B}} \cdot \tilde{\boldsymbol{I}}
\end{aligned}
$$

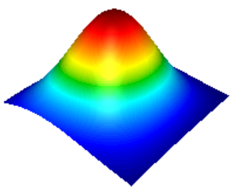

source $\sin(z)\sin(x)$

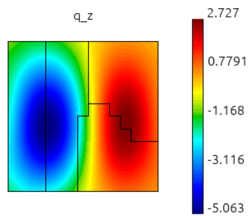

z flux component

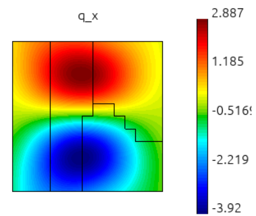

x flux component

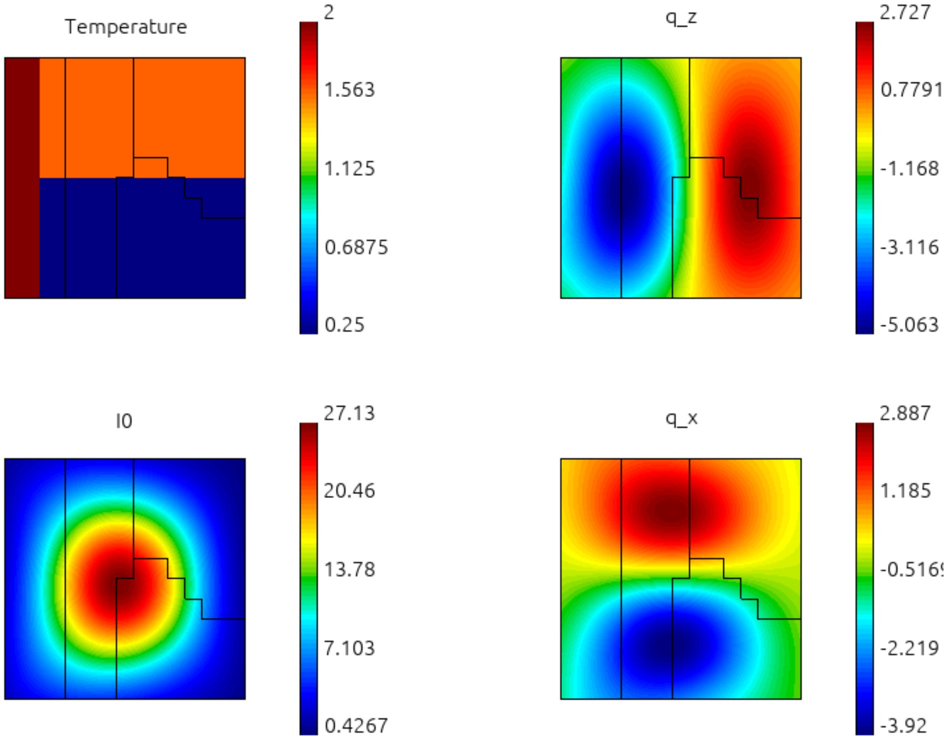
Temperature
2
1.563
1.125
0.6875
0.25
q_z
2.727
0.7791
-1.168
-3.116
-5.063
I0
27.13
20.46
13.78
7.103
0.4267
q_x
2.887
1.185
-0.516
-2.219
-3.92

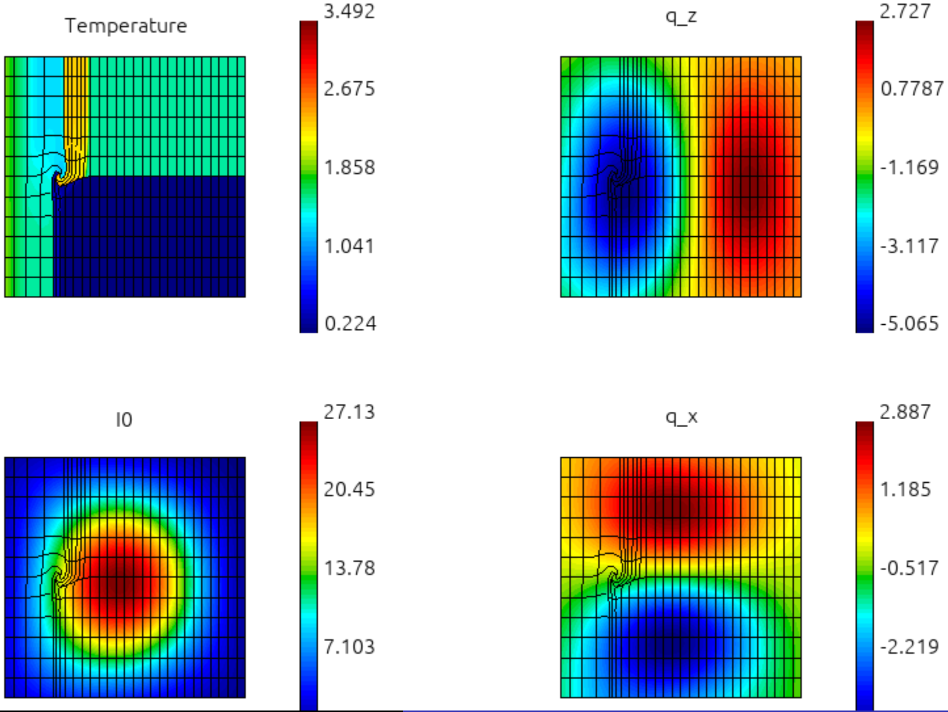
Temperature
3.492
2.675
1.858
1.041
0.224
q_z
2.727
0.7787
-1.169
-3.117
-5.065
I0
27.13
20.45
13.78
7.103
q_x
2.887
1.185
-0.517
-2.219

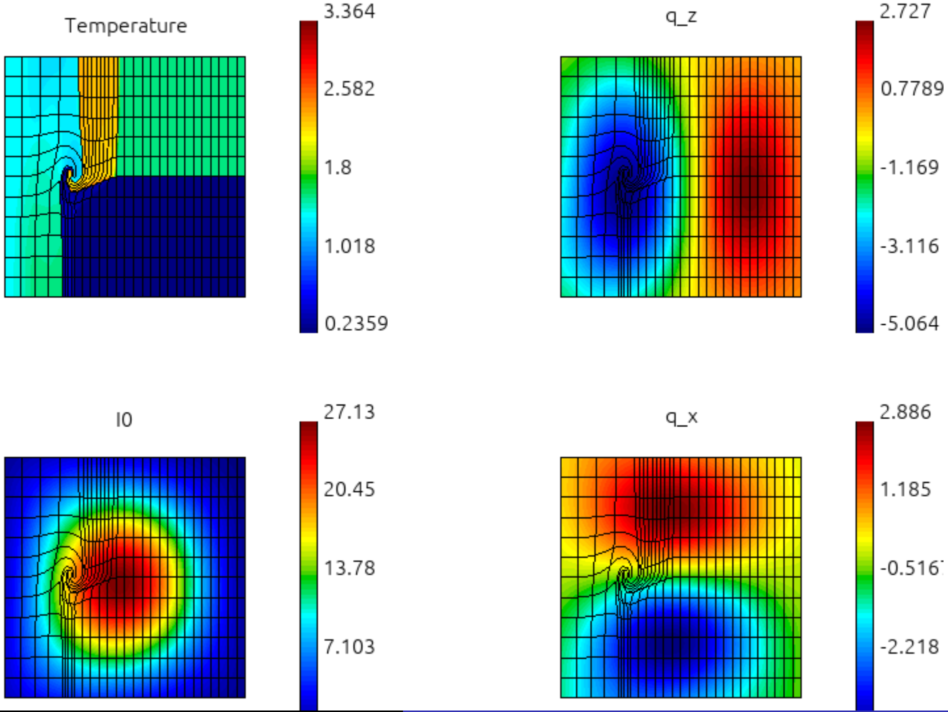
Temperature
3.364
2.582
1.8
1.018
0.2359
q_z
2.727
0.7789
-1.169
-3.116
-5.064
I0
27.13
20.45
13.78
7.103
q_x
2.886
1.185
-0.516
-2.218

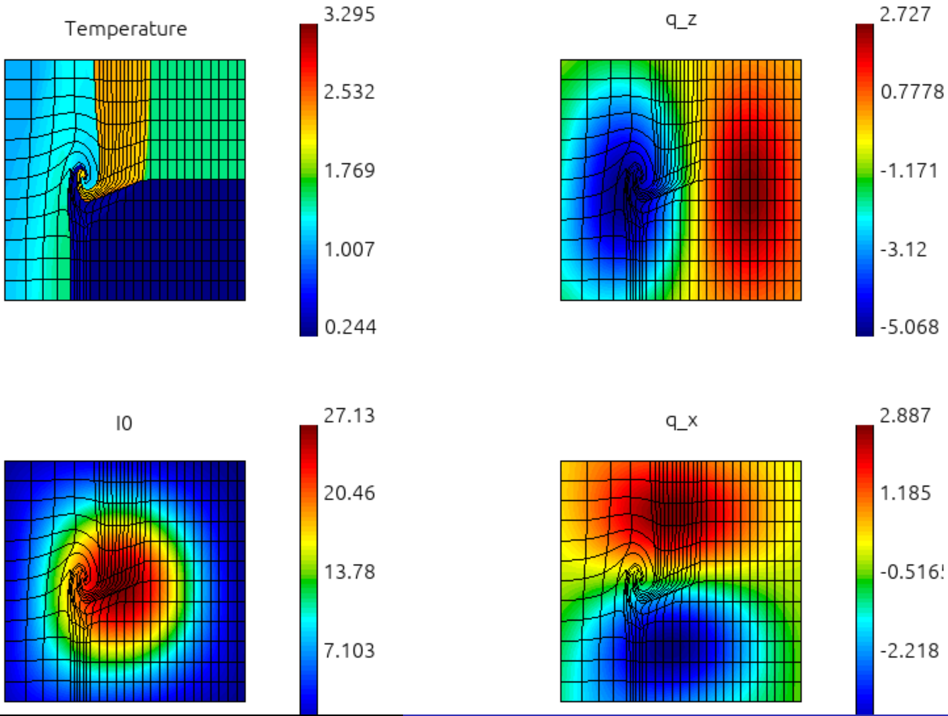
Temperature
3.295
2.532
1.769
1.007
0.244
q_z
2.727
0.7778
-1.171
-3.12
-5.068
I0
27.13
20.46
13.78
7.103
q_x
2.887
1.185
-0.516
-2.218

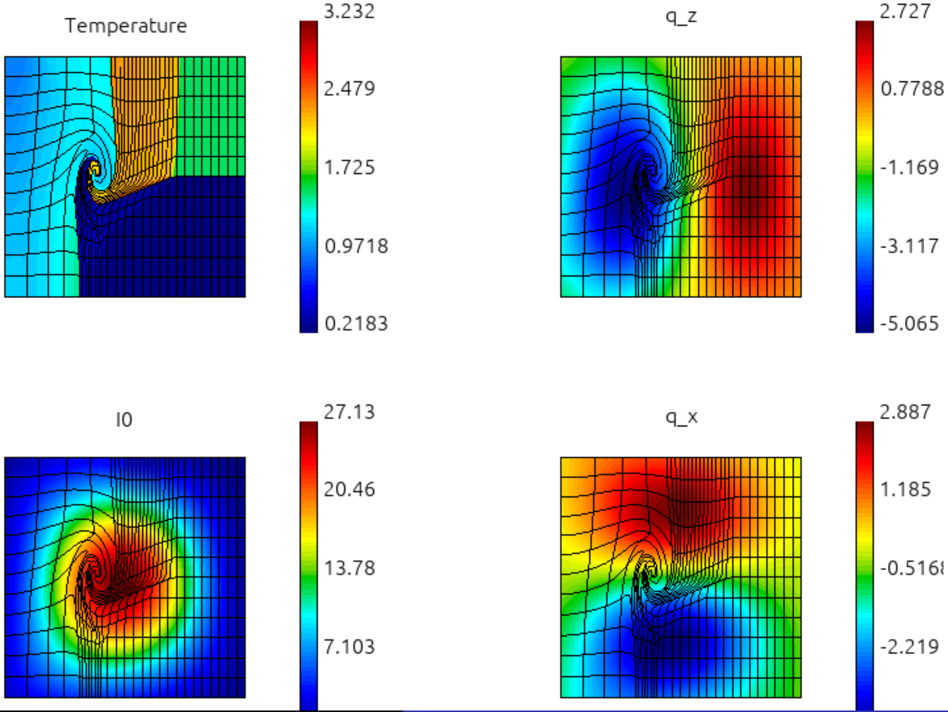
Temperature
3.232
2.479
1.725
0.9718
0.2183
q_z
2.727
0.7788
-1.169
-3.117
-5.065
I0
27.13
20.46
13.78
7.103
q_x
2.887
1.185
-2.219

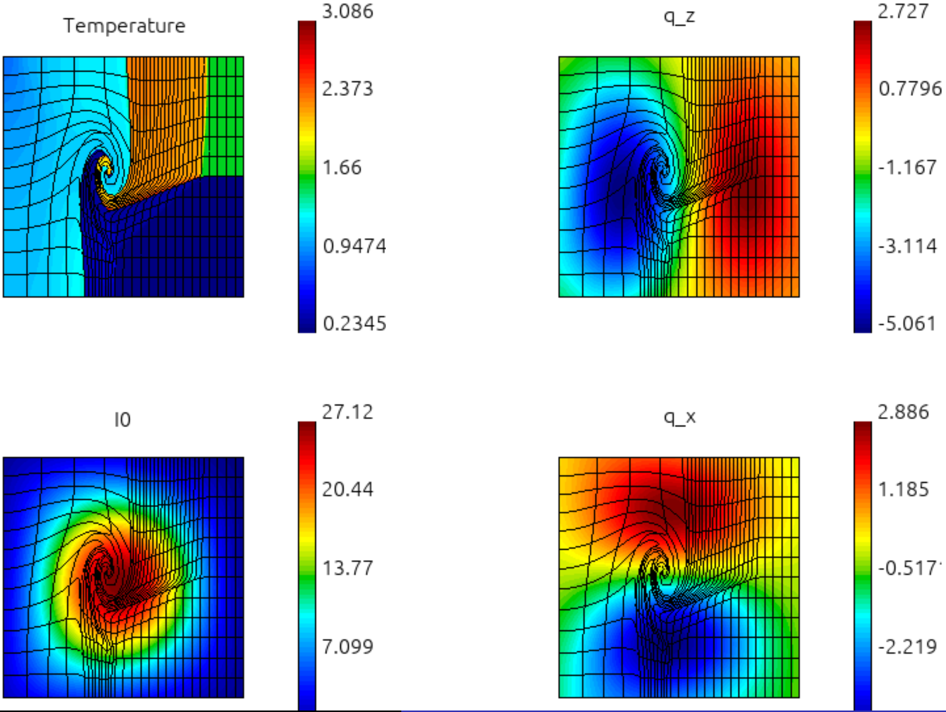
Temperature
3.086
2.373
1.66
0.9474
0.2345
q_z
2.727
0.7796
-1.167
-3.114
-5.061
I0
27.12
20.44
13.77
7.099
q_x
2.886
1.185
-0.517
-2.219

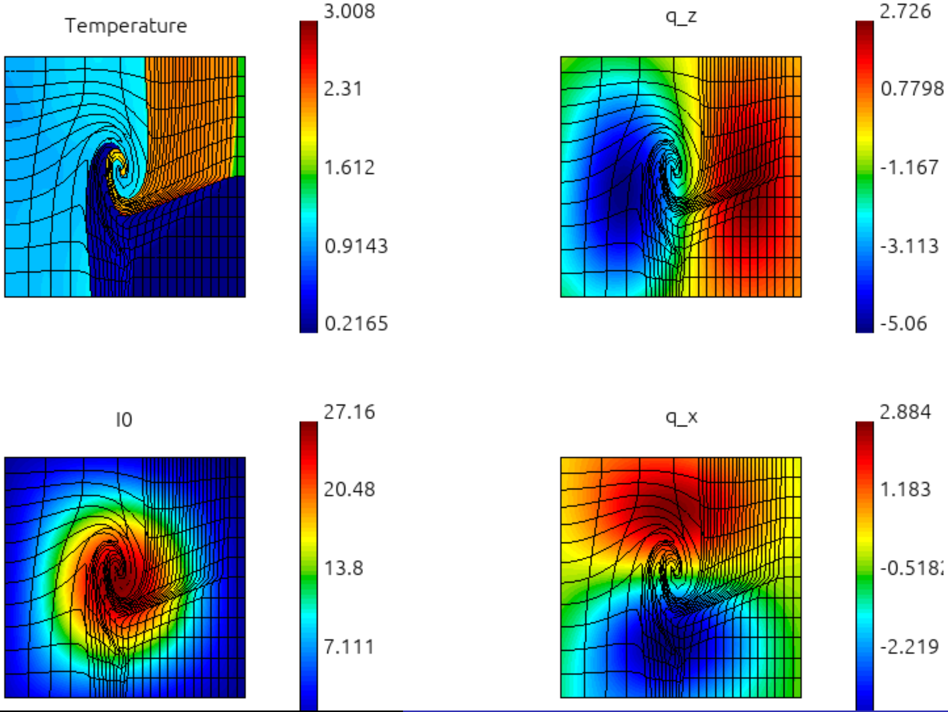
Temperature
3.008
2.31
1.612
0.9143
0.2165
q_z
2.726
0.7798
-1.167
-3.113
-5.06
I0
27.16
20.48
13.8
7.111
q_x
2.884
1.183
-2.219

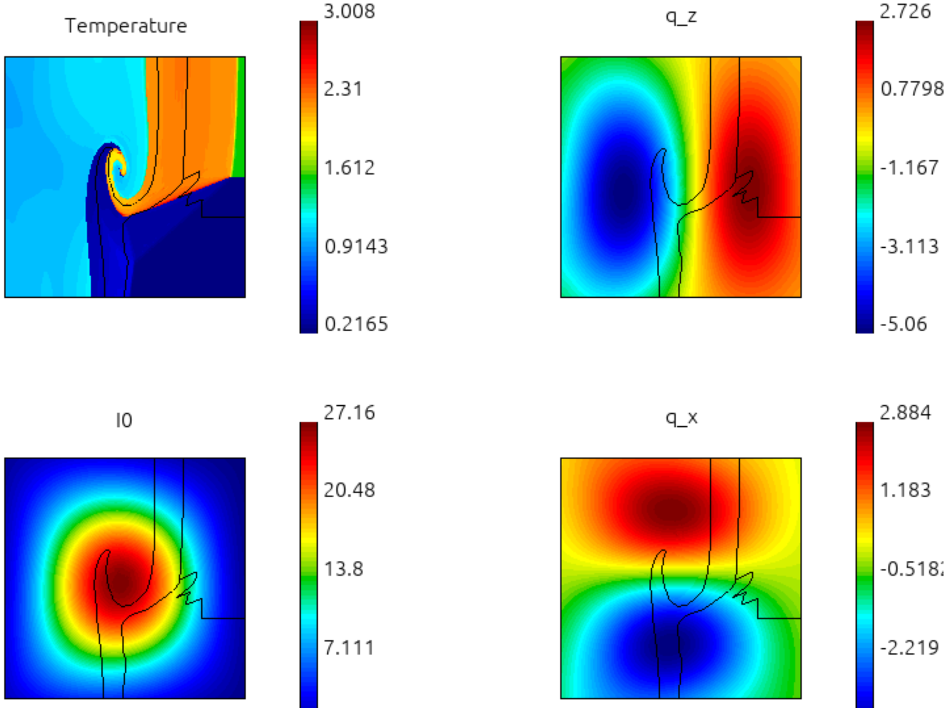
Temperature
3.008
2.31
1.612
0.9143
0.2165
q_z
2.726
0.7798
-1.167
-3.113
-5.06
I0
27.16
20.48
13.8
7.111
q_x
2.884
1.183
-2.219

Curvilinear Framework of Nonlocal Transport

Axisymmetric transport equation

$$\sin(\phi)\left(\cos(\theta)\frac{\partial I}{\partial r} - \frac{\sin(\theta)}{r}\frac{\partial I}{\partial \theta}\right) + \cos(\phi)\frac{\partial I}{\partial z} = S_T\, T_e - \left(k + \sigma - \sin(\phi)\cos(\theta)E_r - \cos(\phi)E_z\right) I + \sigma I_0$$

$$\mathbf{D}\cdot \boldsymbol{I} = \mathbf{S}\cdot \boldsymbol{T} - \left((k+\sigma)\mathbf{M} + \boldsymbol{E}\cdot\mathbf{M}_{\boldsymbol{n}} - \sigma\mathbf{MI}\right)\cdot \boldsymbol{I} + \mathbf{B}\cdot\boldsymbol{I} - \tilde{\mathbf{B}}\cdot\tilde{\boldsymbol{I}}$$

[3]

- high-order curvilinear divergence matrix

$$\mathbf{D} = \int_0^\pi \int_0^\pi \int_\Omega (\boldsymbol{\omega}_\theta \otimes \boldsymbol{\omega}_\phi \otimes \boldsymbol{\psi}) \otimes \left(\sin(\phi)\,\boldsymbol{\omega}_\phi \otimes \left(\cos(\theta)\,\boldsymbol{\omega}_\theta^T \otimes \frac{\partial \boldsymbol{\psi}^T}{\partial r} - \frac{\sin(\theta)}{r}\frac{\partial \boldsymbol{\omega}_\theta^T}{\partial \theta}\otimes\boldsymbol{\psi}^T\right) + \boldsymbol{\omega}_\theta^T \otimes \cos(\phi)\,\boldsymbol{\omega}_\phi^T \otimes \frac{\partial \boldsymbol{\psi}^T}{\partial z}\right) r\,\sin(\phi)\mathrm{d}\Omega\mathrm{d}\phi\mathrm{d}\theta$$

- high-order curvilinear numerical flux matrix

$$\mathbf{B} = \int_0^\pi \int_0^\pi \int_{\Gamma_{\boldsymbol{n}\cdot\boldsymbol{n}_\Gamma < 0}} (\boldsymbol{\omega}_\theta \otimes \boldsymbol{\omega}_\phi \otimes \boldsymbol{\psi}) \otimes (\boldsymbol{\omega}_\theta \otimes \boldsymbol{\omega}_\phi \otimes \boldsymbol{\psi})^T \left(\sin(\phi)\cos(\theta) n_{\Gamma_r} + \cos(\phi) n_{\Gamma_z}\right) r\,\sin(\phi)\mathrm{d}\Gamma\mathrm{d}\phi\mathrm{d}\theta$$

- proper treatment of Lorentz force

$$\boldsymbol{E}\cdot\boldsymbol{n}\frac{\partial I}{\partial|\boldsymbol{v}|} + (\boldsymbol{E} + \boldsymbol{n}\times\boldsymbol{B})\cdot\nabla_{\boldsymbol{n}} I = \begin{bmatrix} E_x \\ E_y \\ E_z \end{bmatrix}^T \cdot \begin{bmatrix} \cos(\theta)\sin(\phi) \\ \sin(\theta)\sin(\phi) \\ \cos(\phi) \end{bmatrix} \frac{\partial I}{\partial |\boldsymbol{v}|} + \left(\begin{bmatrix} E_x \\ E_y \\ E_z \end{bmatrix} + \begin{bmatrix} \cos(\theta)\sin(\phi) \\ \sin(\theta)\sin(\phi) \\ \cos(\phi) \end{bmatrix} \times \begin{bmatrix} B_x \\ B_y \\ B_z \end{bmatrix} \right)^T \cdot \begin{bmatrix} \cos(\phi)\frac{\partial I}{\partial \phi} \\ \frac{1}{\sin(\phi)}\frac{\partial I}{\partial \theta} \\ -\sin(\phi)\frac{\partial I}{\partial \phi} \end{bmatrix}$$

[3] mfem.org – "My finite element library is higher order than yours..."

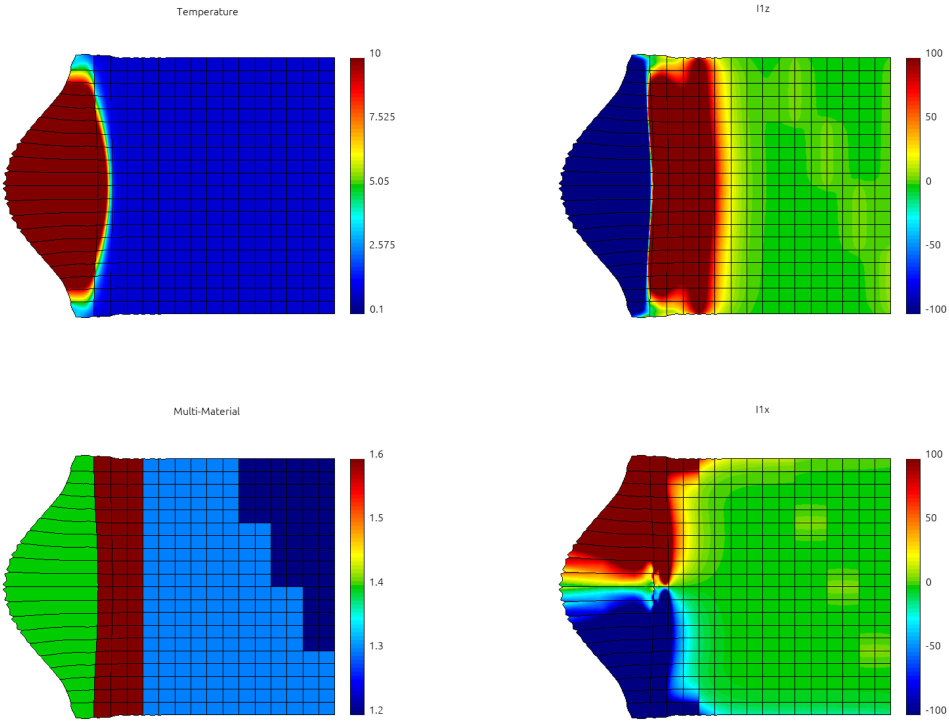
Temperature
10
7.525
5.05
2.575
0.1
I1z
100
50
0
-50
-100
Multi-Material
1.6
1.5
1.4
1.3
1.2
I1x
100
50
0
-50
-100

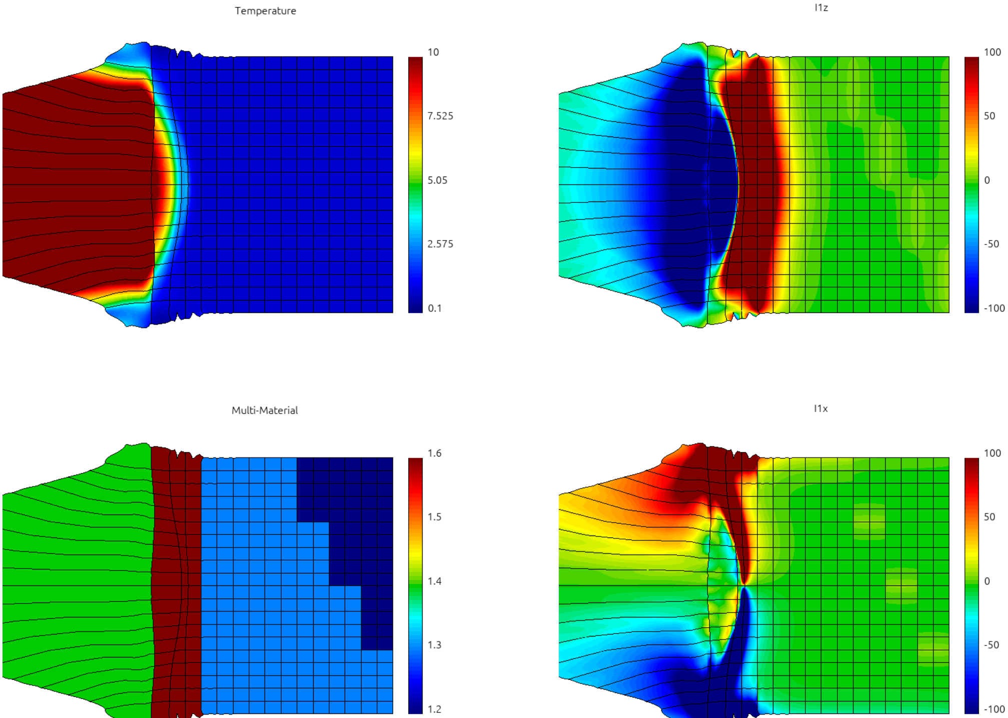
Temperature
10
7.525
5.05
2.575
0.1
I1z
100
50
0
-50
-100
Multi-Material
1.6
1.5
1.4
1.3
1.2
I1x
100
50
0
-50
-100

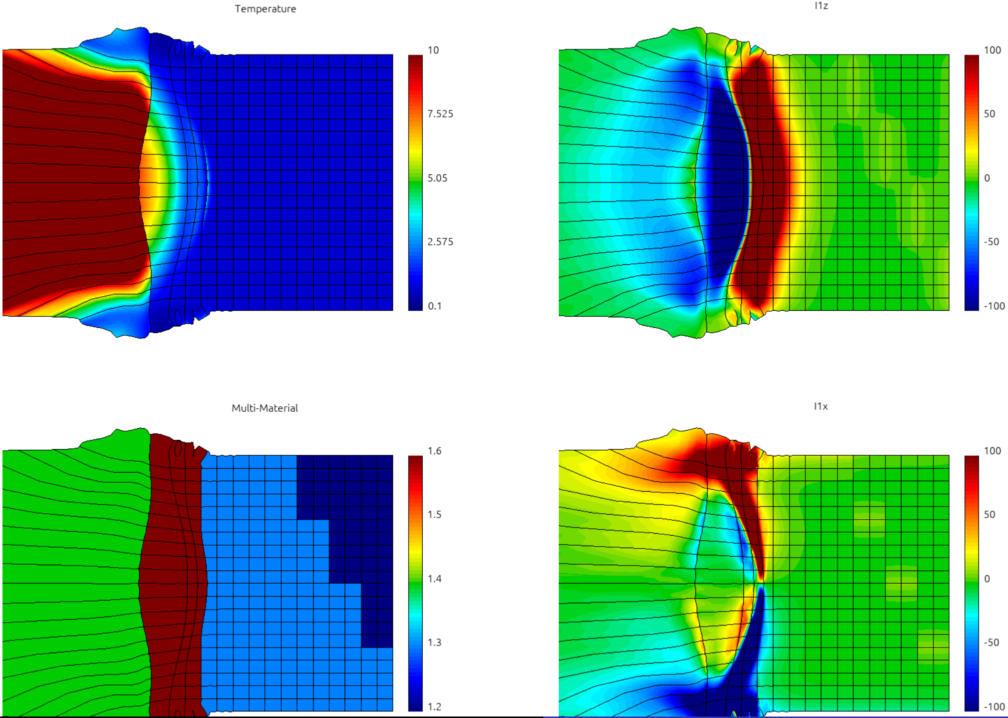
Temperature
10
7.525
5.05
2.575
0.1
I1z
100
50
0
-50
-100
Multi-Material
1.6
1.5
1.4
1.3
1.2
I1x
100
50
0
-50
-100

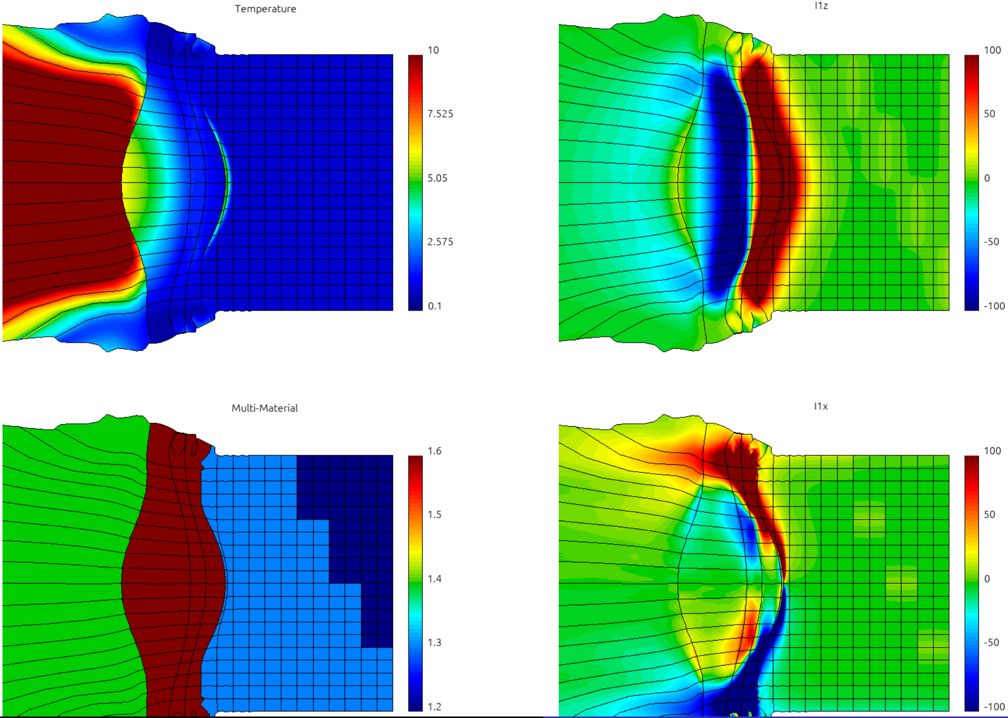
Temperature
10
7.525
5.05
2.575
0.1
I1z
100
50
0
-50
-100
Multi-Material
1.6
1.5
1.4
1.3
1.2
I1x
100
50
0
-50
-100

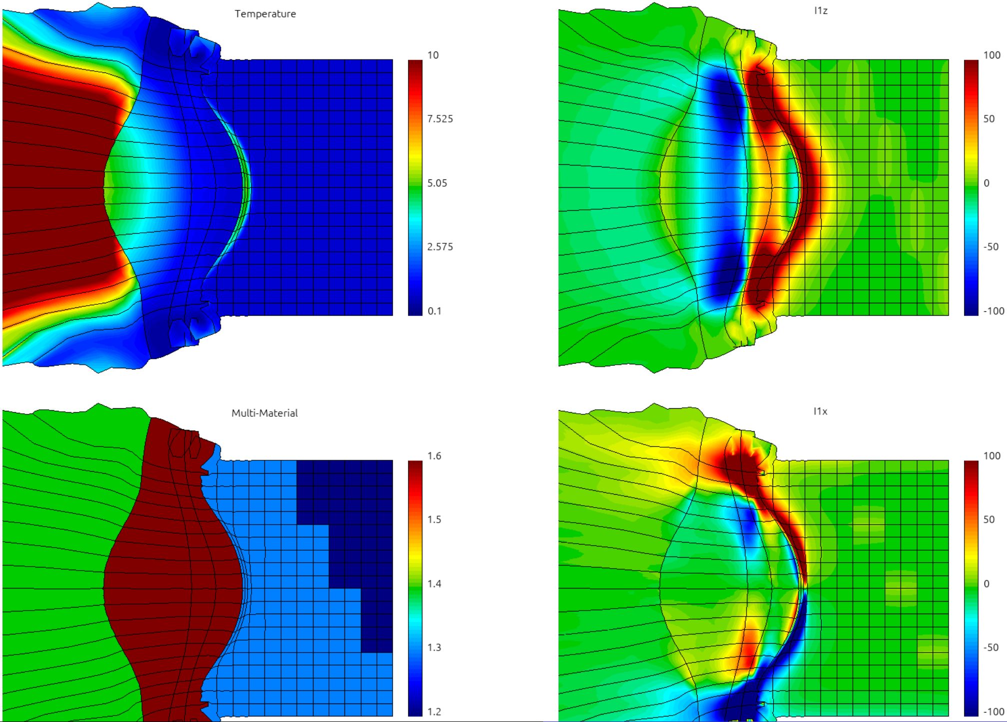
Temperature
10
7.525
5.05
2.575
0.1
I1z
100
50
0
-50
-100
Multi-Material
1.6
1.5
1.4
1.3
1.2
I1x
100
50
0
-50
-100

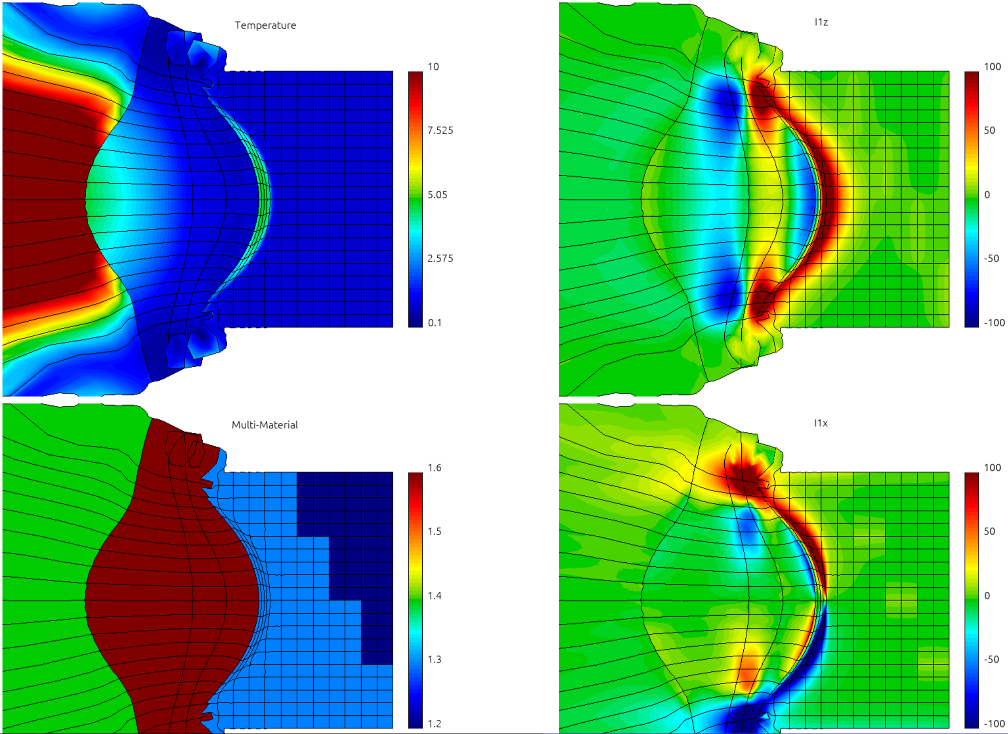
Temperature
10
7.525
5.05
2.575
0.1
I1z
100
50
0
-50
-100
Multi-Material
1.6
1.5
1.4
1.3
1.2
I1x
100
50
0
-50
-100

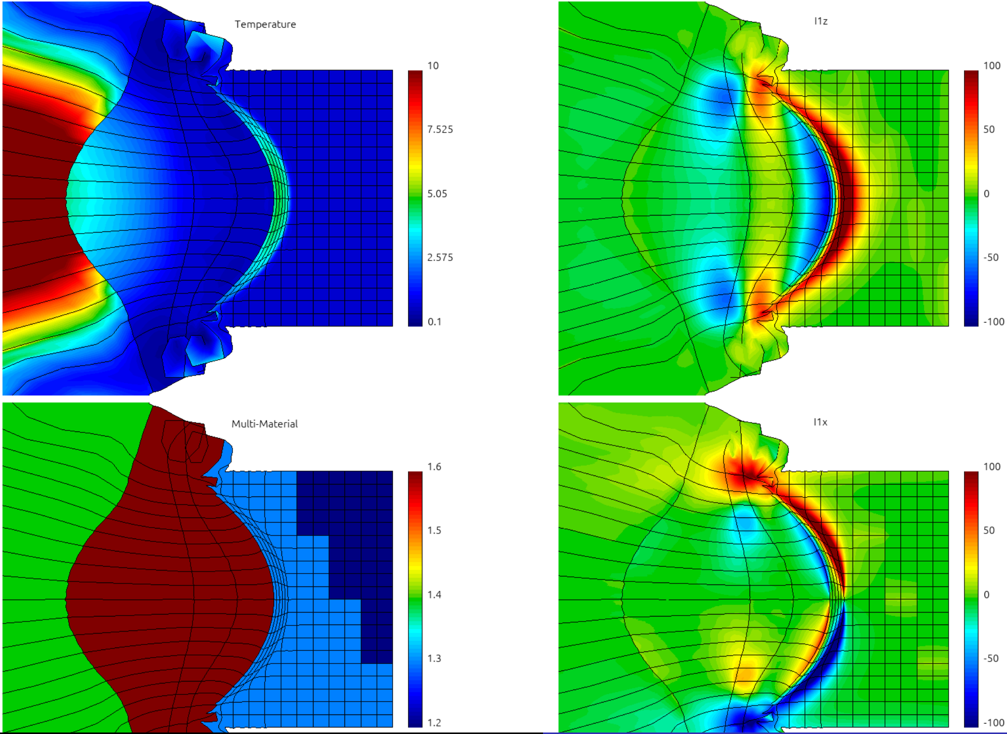
Temperature
10
7.525
5.05
2.575
0.1
I1z
100
50
0
-50
-100
Multi-Material
1.6
1.5
1.4
1.3
1.2
I1x
100
50
0
-50
-100

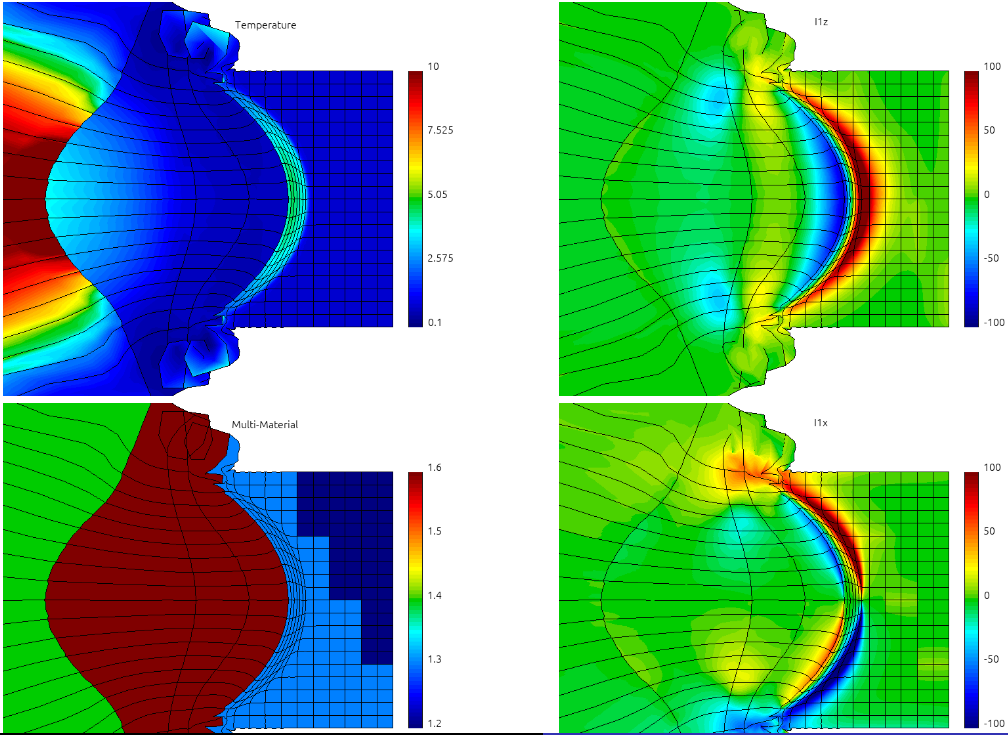
Temperature
10
7.525
5.05
2.575
0.1
I1z
100
50
0
-50
-100
Multi-Material
1.6
1.5
1.4
1.3
1.2
I1x
100
50
0
-50
-100

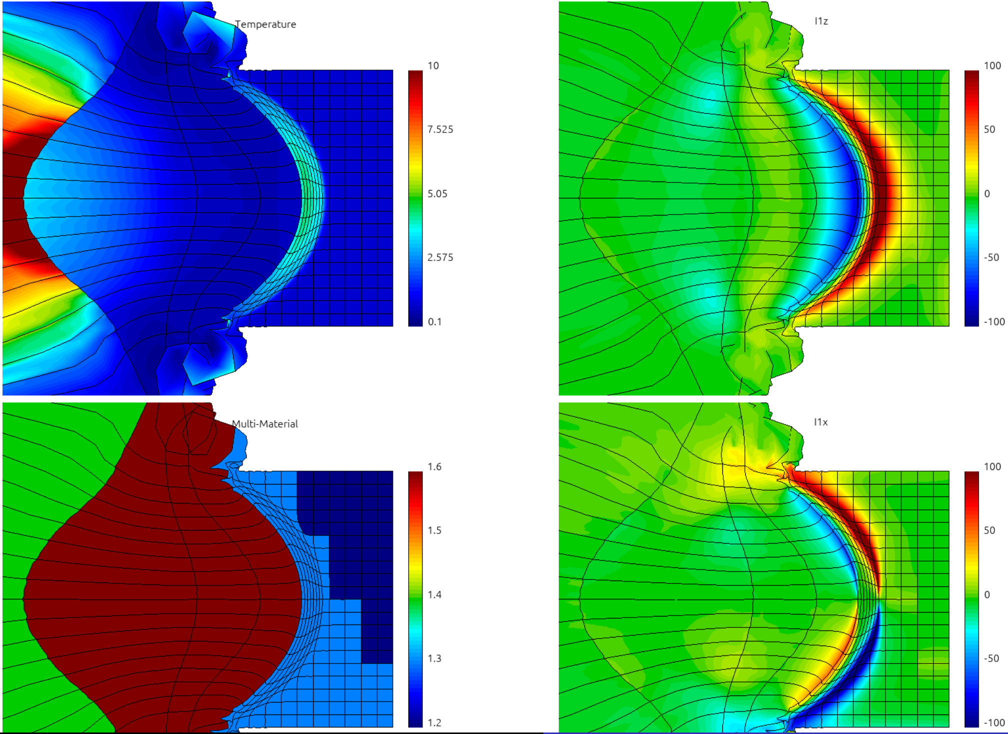
Temperature
10
7.525
5.05
2.575
0.1
I1z
100
50
0
-50
-100
Multi-Material
1.6
1.5
1.4
1.3
1.2
I1x
100
50
0
-50
-100

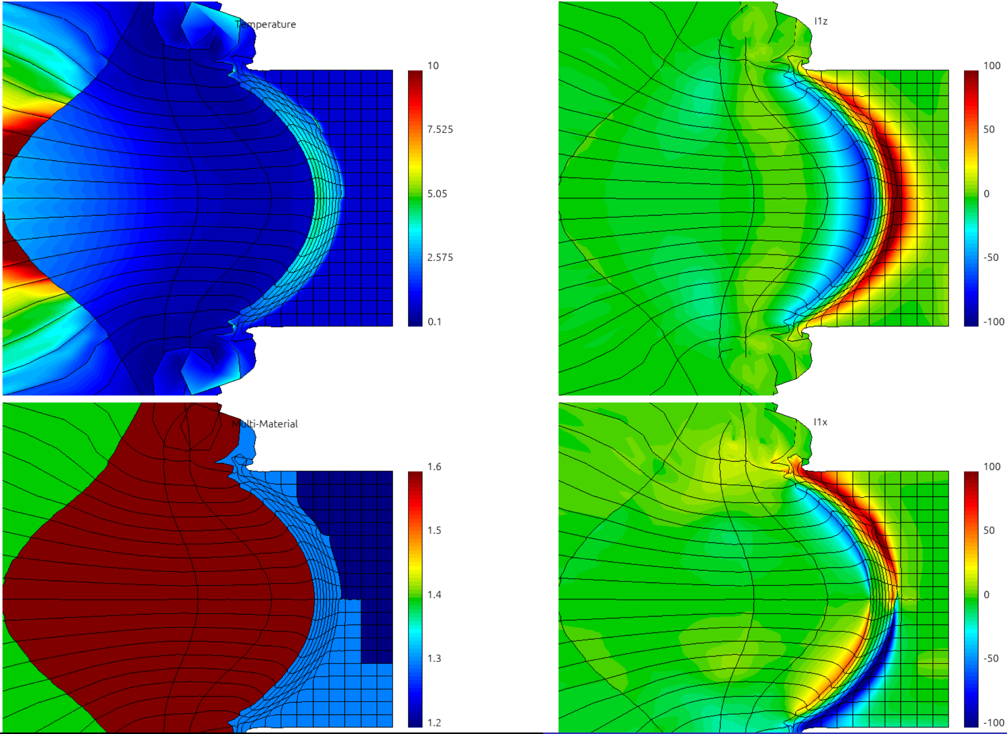
Temperature
10
7.525
5.05
2.575
0.1
I1z
100
50
0
-50
-100
Multi-Material
1.6
1.5
1.4
1.3
1.2
I1x
100
50
0
-50
-100

Laghos + DG-BGK&T

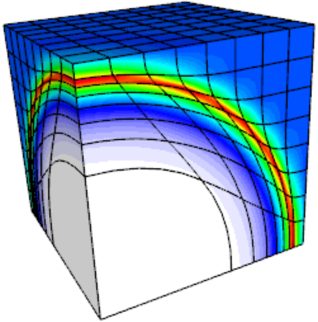

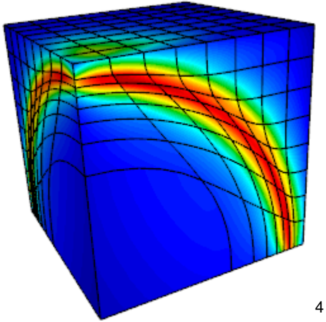

4

[4] https://github.com/homijan/NTH-Laghos

Hotspot relaxation

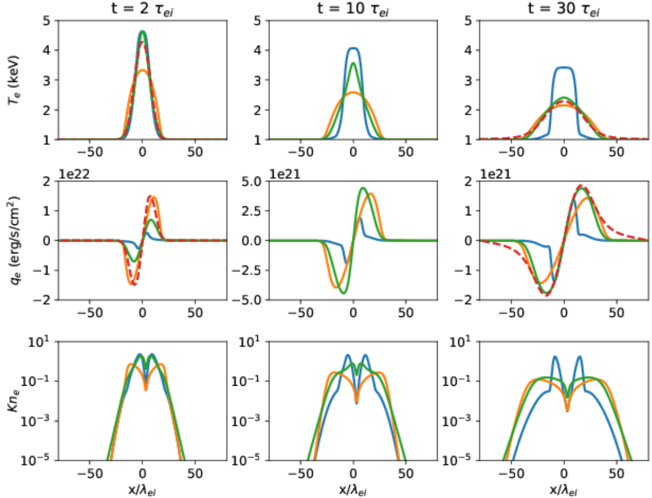

Figure : Green - NTH, red - Fokker-Planck, yellow - SH, blue - flux limited SH.

5

[5] M. Holec, J. Nikl, and S. Weber, ”Nonlocal Transport Hydrodynamic Model for Laser Heated Plasmas”, *Phys. Plasmas*, submitted (2017).

Short-Epperlein test

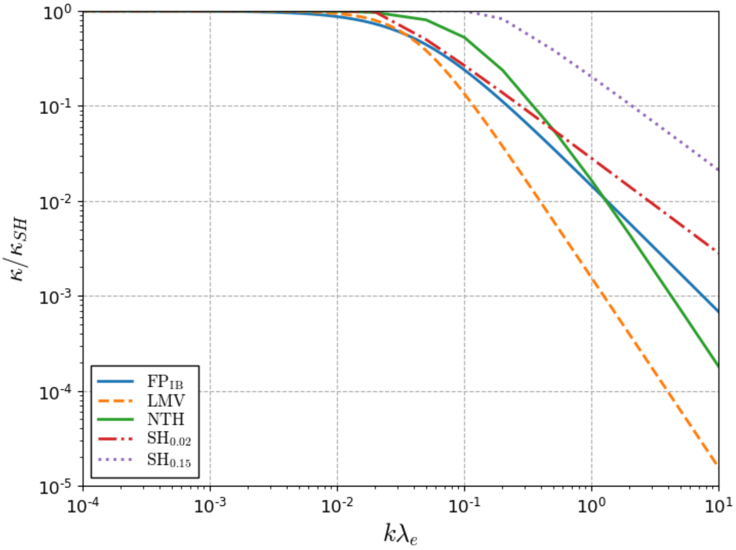

[5] M. Holec, J. Nikl, and S. Weber, "Nonlocal Transport Hydrodynamic Model for Laser Heated Plasmas", *Phys. Plasmas*, submitted (2017).

Planar plastic target irradiated by NIF laser pulse

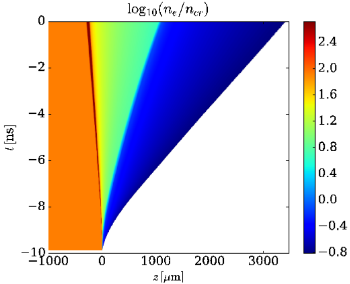

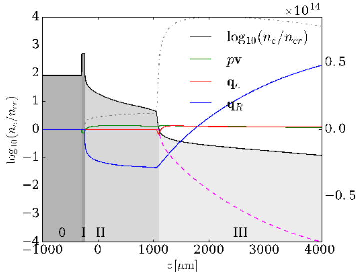

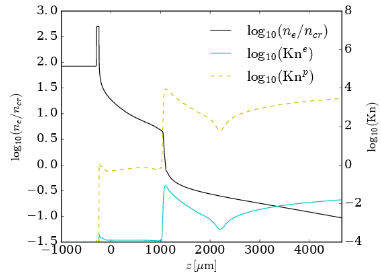

The nonlocal transport of energy leads to generation of *conduction zone* (turquoise color), whose thickness is one of the main parameters for the seeding of Rayleigh-Taylor and Richtmyer-Meshkov instabilities.

[5] M. Holec, J. Nikl, and S. Weber, "Nonlocal Transport Hydrodynamic Model for Laser Heated Plasmas", *Phys. Plasmas*, submitted (2017).

Preheat observed in a shocked CH foam at OMEGA facility

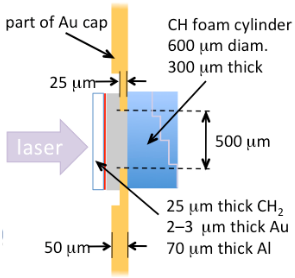

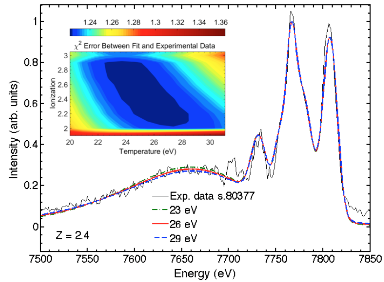

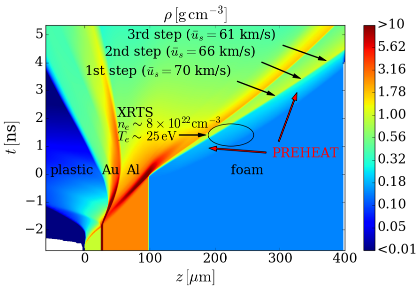

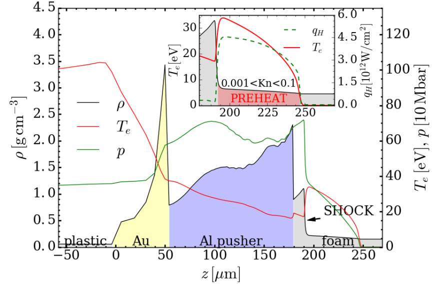

flat 2 ns laser pulse, $8{\times}10^{14}$ Wcm2, 300 μm thick foam ($\rho = 0.13$ g/cm^3)

6

[6] K. Falk, M. Holec, C. J. Fontes et al, "Measurement of preheat due to nonlocal electron transport in warm dense matter", *Phys. Rev. Lett.* 120, 025002 (2018).

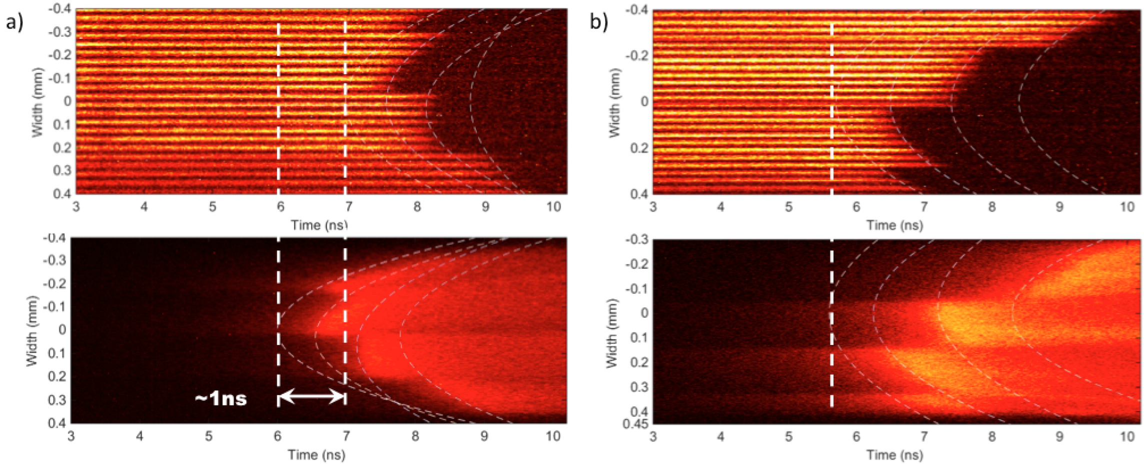

a) recent experiment with new phase-plates, b) previous experiment

[6] K. Falk, M. Holec, C. J. Fontes et al, "Measurement of preheat due to nonlocal electron transport in warm dense matter", *Phys. Rev. Lett.* 120, 025002 (2018).

VISAR oscillations

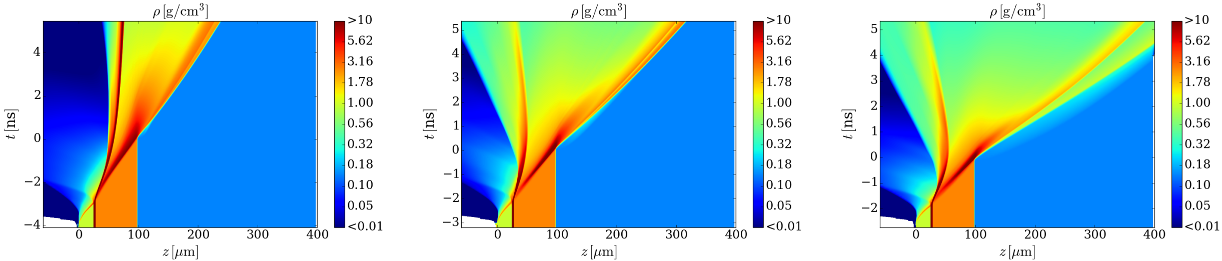

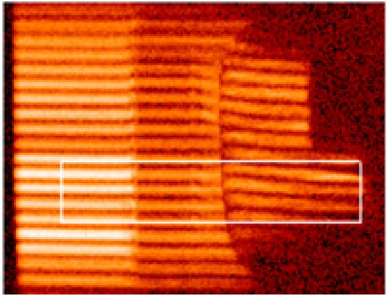

7

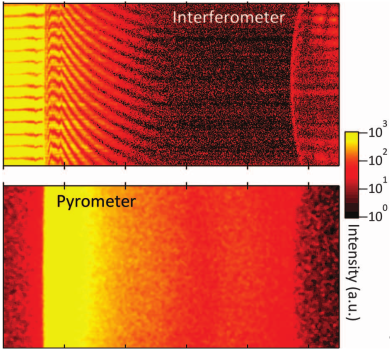

8

---

[7]K. Falk et al, *Phys. Plas.*, 21, 056309 (2014).
[8]R. S. Williams et al, *Science*, 338, 1330 (2012).

Nonlocal vs. SH diffusion

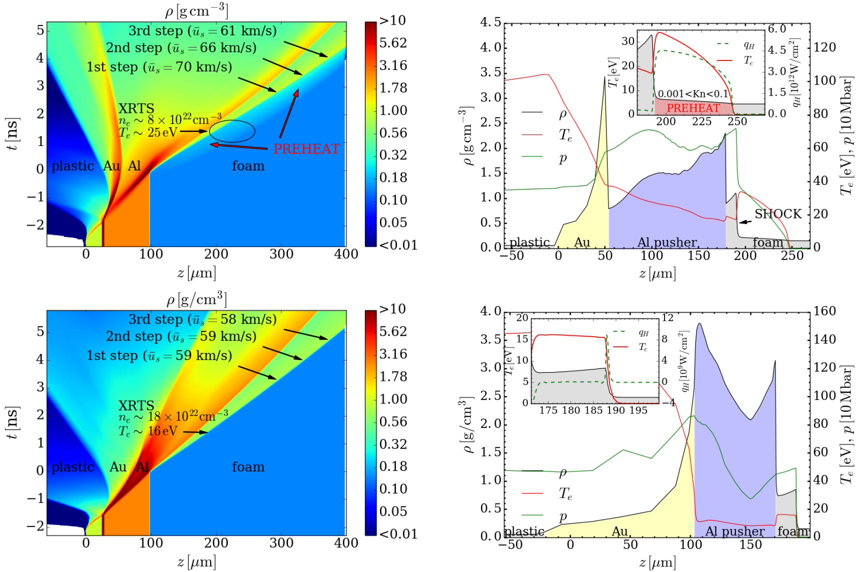

Effective mean free path was $4.1 \times v_T$, according to LANL code ATOMIC the mean free path in WDM foam increases $\approx 30\%$.

[8] K. Falk, M. Holec, C. J. Fontes et al, "Measurement of preheat due to nonlocal electron transport in warm dense matter", *Phys. Rev. Lett.* 120, 025002 (2018).

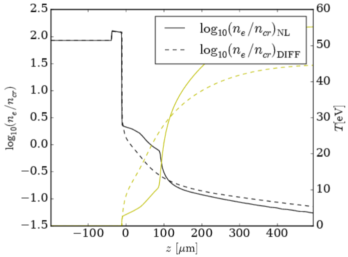

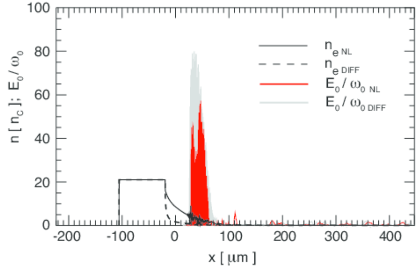

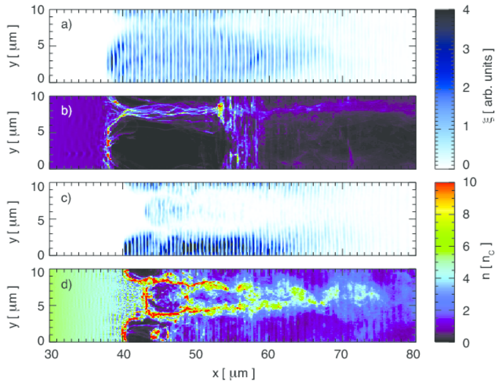

[9]

[9]M. Holec,J. Nikl, and M. Vranic, ”The effect of pre-plasma formation under nonlocal transport conditions for ultra-relativistic laser-plasma interaction”, *Plasma Phys. Control. Fusion*, submitted (2017).

Example of moment methods

AWBS Boltzmann transport equation

$$\boldsymbol{n} \cdot \nabla f + \frac{1}{v} \left(\boldsymbol{E} + v \boldsymbol{n} \times \boldsymbol{B} \right) \cdot \nabla_{\boldsymbol{v}} f = \frac{v}{\lambda} \frac{\partial}{\partial v} \left(f - f_M \right) + \frac{1}{2 \lambda_{ei}} \frac{\partial}{\partial \mu} \left((1 - \mu^2) \frac{\partial f}{\partial \mu} \right).$$

M1-AWBS transport model

$$\begin{aligned}
\nu_e v \frac{\partial}{\partial v} \left(f_0 - f_M \right) &= v \nabla \cdot \boldsymbol{f}_1 + \frac{q_e}{m_e v^2} \boldsymbol{E} \cdot \frac{\partial}{\partial v} \left(v^2 \boldsymbol{f}_1 \right), \\
\nu_e v \frac{\partial}{\partial v} \boldsymbol{f}_1 - \nu_t \boldsymbol{f}_1 &= v \nabla \cdot (\mathbf{A} f_0) + \frac{q_e}{m_e v^2} \boldsymbol{E} \cdot \frac{\partial}{\partial v} \left(v^2 \mathbf{A} f_0 \right) + \frac{q_e}{m_e v} \boldsymbol{E} \cdot (\mathbf{A} - \mathbf{I}) f_0 + \frac{q_e}{m_e c} \boldsymbol{B} \times \boldsymbol{f}_1.
\end{aligned}$$

High-order finite element bilienar form integrators

$$\boldsymbol{\mathcal{M}}^0_{(g)} = \int_\Omega \phi \otimes \phi^T g \, \mathrm{d}\Omega, \quad \boldsymbol{\mathcal{M}}^1_{(g)} = \int_\Omega \mathbf{w} \cdot \mathbf{w}^T g \, \mathrm{d}\Omega, \quad \boldsymbol{\mathcal{D}}_{(\mathbf{G})} = \int_\Omega \mathbf{G} : \nabla \mathbf{w} \otimes \phi^T \, \mathrm{d}\Omega,$$

$$\boldsymbol{\mathcal{V}}_{(\boldsymbol{g})} = \int_\Omega \mathbf{w} \cdot \boldsymbol{g} \otimes \phi^T \, \mathrm{d}\Omega, \quad \boldsymbol{\mathcal{B}}_{(\boldsymbol{g})} = \int_\Omega \mathbf{w} \cdot \boldsymbol{g} \times \mathbf{w}^T \, \mathrm{d}\Omega,$$

$$\left(\boldsymbol{\mathcal{M}}^0_{(\nu_e)} - \boldsymbol{\mathcal{M}}^0_{\left(\frac{1}{v\boldsymbol{f}_0^n}\tilde{\boldsymbol{E}}^T\cdot\boldsymbol{f}_1^n\right)}\right)\cdot\frac{d\boldsymbol{f}_0}{dv}^{*} = \boldsymbol{\mathcal{D}}^T_{(\mathbf{I})}\cdot\boldsymbol{f}_1^n + \boldsymbol{\mathcal{V}}^T_{(2\tilde{\boldsymbol{E}}/v^2)}\cdot\boldsymbol{f}_1^n + \boldsymbol{\mathcal{M}}^0_{(\nu_e)}\cdot\frac{\partial\boldsymbol{f}_M}{\partial v}$$

$$\boldsymbol{\mathcal{M}}^1_{(\nu_e)}\cdot\frac{d\boldsymbol{f}_1}{dv} = -\boldsymbol{\mathcal{D}}_{(\mathbf{A})}\cdot\boldsymbol{f}_0^n + \boldsymbol{\mathcal{V}}_{(\mathbf{A}\cdot\tilde{\boldsymbol{E}}/v)}\cdot\frac{d\boldsymbol{f}_0}{dv}^{*} + \boldsymbol{\mathcal{V}}_{((3\mathbf{A}-\mathbf{I})\cdot\tilde{\boldsymbol{E}}/v^2)}\cdot\boldsymbol{f}_0^n + \boldsymbol{\mathcal{B}}_{(\tilde{\boldsymbol{B}}/v)}\cdot\boldsymbol{f}_1^n + \boldsymbol{\mathcal{M}}^1_{(\nu_t/v)}\cdot\boldsymbol{f}_1^n$$

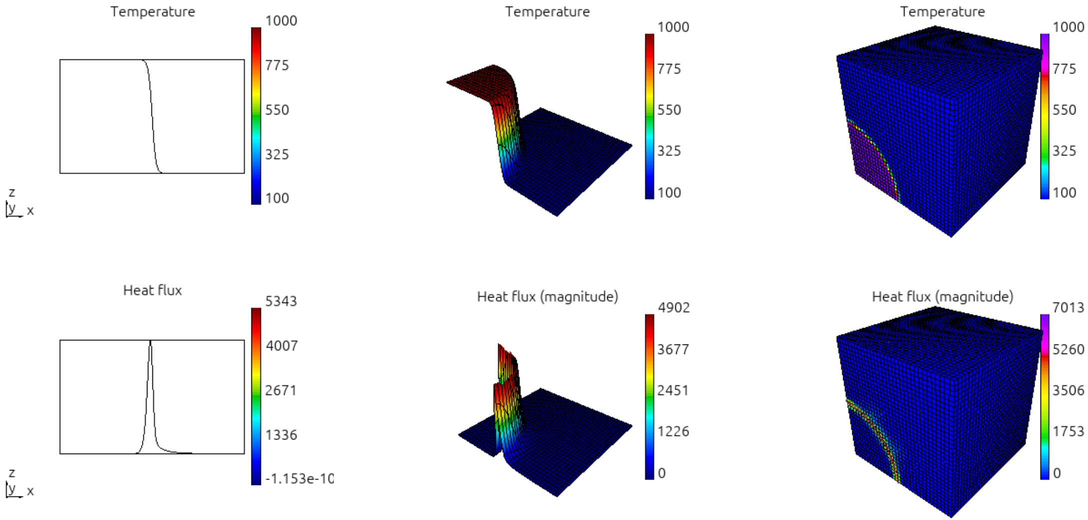

Nonlocal Transport Magneto-Hydrodynamic model

$$\boldsymbol{n}\cdot\nabla_{\boldsymbol{x}} f + \frac{1}{|\boldsymbol{v}|}\left(\boldsymbol{E}+\boldsymbol{v}\times\boldsymbol{B}\right)\cdot\nabla_{\boldsymbol{v}} f = \frac{f_{MB}(|\boldsymbol{v}|,T_e)-f}{\lambda_{ei}(|\boldsymbol{v}|^4)} \rightarrow \mathbf{D}\cdot\boldsymbol{f} + \frac{1}{|\boldsymbol{v}|}\boldsymbol{E}\cdot\mathbf{V}_E\cdot\boldsymbol{f} + \mathbf{B}\times\mathbf{V}_B\cdot\boldsymbol{f} = \boldsymbol{S} - k_{|\boldsymbol{v}|}\mathbf{M}\cdot\boldsymbol{f}$$

NTH Electric field vs. generalized Ohm's law

$$\boldsymbol{E} = \frac{1}{en_e}\left(\boldsymbol{R}_T - \nabla p_e\right) + \frac{\boldsymbol{j}}{en_e\sigma} + \frac{1}{en_e c}\boldsymbol{j}\times\boldsymbol{B}$$

$$\boldsymbol{E}\cdot\sum_{\Delta v^g}\int_{4\pi}\mathbf{V}_E\cdot\boldsymbol{f} = -\sum_{\Delta v^g}\int_{4\pi}\mathbf{D}\cdot|\boldsymbol{v}|\boldsymbol{f} - \sum_{\Delta v^g}\int_{4\pi}k_{|\boldsymbol{v}|}\mathbf{M}\cdot|\boldsymbol{v}|\boldsymbol{f} - \sum_{\Delta v^g}\int_{4\pi}\mathbf{B}\times\mathbf{V}_B\cdot|\boldsymbol{v}|\boldsymbol{f}$$

$$\nabla\times\boldsymbol{E} = -\frac{1}{c}\frac{\partial\boldsymbol{B}}{\partial t} \qquad \text{(life of magnetic field}\boldsymbol{B}\text{)}$$

$$\nabla\times\boldsymbol{B} = \frac{4\pi}{c}\left(\boldsymbol{j}+\tilde{\boldsymbol{j}}\right) \qquad \text{(quasi-neutrality}\nabla\cdot\left(\boldsymbol{j}+\tilde{\boldsymbol{j}}\right)=0\text{)}$$

Applying generalized Ohm's and Ampere's laws, we get

$$\nabla\times\boldsymbol{E} = \nabla\times\left(\frac{1}{en_e}\left(\boldsymbol{R}_T-\nabla p_e\right) + \frac{c}{en_e\sigma 4\pi}\nabla\times\boldsymbol{B} - \frac{\tilde{\boldsymbol{j}}}{en_e\sigma} + \frac{1}{en_e c}\boldsymbol{j}\times\boldsymbol{B}\right)$$

Maxwell Equations for Hydrodynamics - dynamo equation for nonlocal magnetic field source

$$\frac{1}{c}\frac{\partial\boldsymbol{B}}{\partial t} = -\nabla\times\frac{1}{en_e c}\boldsymbol{j}\times\boldsymbol{B} - \nabla\times\frac{c}{en_e\sigma 4\pi}\nabla\times\boldsymbol{B} - \nabla\times\left(\frac{\sum_{\Delta v^g}\int_{4\pi}\mathbf{D}\cdot|\boldsymbol{v}|\boldsymbol{f}}{\sum_{\Delta v^g}\int_{4\pi}\mathbf{V}_E\cdot\boldsymbol{f}} + \frac{\tilde{\boldsymbol{j}}}{en_e\sigma}\right)$$

Nonlocal Transport Magneto-Hydrodynamics

$$
\begin{aligned}
\frac{\mathrm{d}\rho}{\mathrm{d}t} &= -\rho\nabla\cdot\boldsymbol{u}\,,\\
\rho\frac{\mathrm{d}\boldsymbol{u}}{\mathrm{d}t} &= -\nabla(p_i+p_e)\,,\\
\rho\left(\frac{\partial\varepsilon_i}{\partial T_i}\frac{\mathrm{d}T_i}{\mathrm{d}t}+\frac{\partial\varepsilon_i}{\partial\rho}\frac{\mathrm{d}\rho}{\mathrm{d}t}\right) &= -p_i\nabla\cdot\boldsymbol{u}-G(T_i-T_e)\,,\\
\rho\left(\frac{\partial\varepsilon_e}{\partial T_e}\frac{\mathrm{d}T_e}{\mathrm{d}t}+\frac{\partial\varepsilon_e}{\partial\rho}\frac{\mathrm{d}\rho}{\mathrm{d}t}\right) &= -p_e\nabla\cdot\boldsymbol{u}-\nabla\cdot(\boldsymbol{q}_e+\boldsymbol{q}_R)+G(T_i-T_e)+Q_{\mathrm{IB}}(\boldsymbol{E}_L)\,,
\end{aligned}
$$

the quantities $\frac{\partial\varepsilon}{\partial\rho}=\frac{\partial f}{\partial\rho}-T\frac{\partial^2 f}{\partial\rho\partial T}$, $\frac{\partial\varepsilon}{\partial T}=-T\frac{\partial^2 f}{\partial T^2}$, $p=\rho^2\frac{\partial f}{\partial\rho}$, $G=\rho\frac{\partial\varepsilon_e}{\partial T_e}\nu_{ei}$ provides our HerEOS equation of state. [10]

Nonlocal transport of photon intensity
$I^p=\int_\nu f^p\frac{h^4\nu^3}{c^2}\,\mathrm{d}\nu$

$$\boldsymbol{n}\cdot\nabla I^p=\frac{aT_e^4-I^p}{\lambda^p}$$

Radiation closure relations

$$\boldsymbol{q}_R=\int_{4\pi}\boldsymbol{n}\,I^p\,\mathrm{d}\boldsymbol{n}\xrightarrow{diffusive}\nabla\cdot\boldsymbol{q}_R=-\nabla\cdot\left(\frac{c}{3\chi_R}\nabla E\right)$$

Nonlocal transport of electron intensity $I^e=\int_\nu f^e\frac{m_e|\boldsymbol{v}|^5}{2}\,\mathrm{d}|\boldsymbol{v}|$

$$\boldsymbol{n}\cdot\nabla f^e+(\boldsymbol{E}+\boldsymbol{v}\times\boldsymbol{B})\cdot\nabla_{\boldsymbol{v}}f^e=\frac{k_B n_e\frac{\sqrt{2}}{\pi^{\frac{3}{2}}}v_{th}T_e\;-\;f^e}{\lambda^e}$$

Electron closure relations

$$\boldsymbol{q}_e=\int_{4\pi}\boldsymbol{n}\,f^e\,\mathrm{d}\boldsymbol{n}\xrightarrow{diffusive}\nabla\cdot\boldsymbol{q}_e=-\nabla\cdot\left(\kappa_{SH}\,T_e^{\frac{5}{2}}\,\nabla T_e\right)$$

$$\frac{1}{c}\frac{\partial\boldsymbol{B}}{\partial t}=-\nabla\times\frac{1}{en_ec}\boldsymbol{j}\times\boldsymbol{B}-\nabla\times\frac{c}{en_e\sigma4\pi}\nabla\times\boldsymbol{B}-\nabla\times\left(\frac{\sum_{\Delta v^g}\int_{4\pi}\mathbf{D}\cdot|\boldsymbol{v}|\boldsymbol{f}}{\sum_{\Delta v^g}\int_{4\pi}\mathbf{V}_E\cdot\boldsymbol{f}}+\frac{\tilde{\boldsymbol{j}}}{en_e\sigma}\right)$$

[10] M. Zeman, M. Holec, P. Vachal, ”HerEOS: a Framework for Consistent Treatment of the Equation of State in ALE Hydrodynamics”, *Comp. Math. Appl.*, submitted (2017).

Conclusions

Plasma Euler and Transport Equations hydro code PETE

$$\frac{\partial \rho}{\partial t} = -\nabla \cdot (\rho \boldsymbol{u}),$$
$$\frac{\partial \rho \boldsymbol{u}}{\partial t} = -\nabla \cdot (\rho \boldsymbol{u} \otimes \boldsymbol{u} + p\mathbf{I}),$$
$$\frac{\partial E}{\partial t} = -\nabla \cdot (E\boldsymbol{u} + p\boldsymbol{u} + \boldsymbol{q}_L + \boldsymbol{q}_e + \boldsymbol{q}_R),$$

density ρ, fluid velocity $\boldsymbol{u}$, total energy $E(T)$, pressure $p(\rho, T)$, laser energy flux $\boldsymbol{q}_L$, electron heat flux $\boldsymbol{q}_e$, radiation flux $\boldsymbol{q}_R$.

$$\boldsymbol{n} \cdot \nabla I^p = \frac{\sigma^p T_e - I^p}{\lambda^p},$$
$$\boldsymbol{q}_R = \int_{4\pi} \boldsymbol{n}\, I^p \, \mathrm{d}\boldsymbol{n},$$

$$\boldsymbol{n} \cdot \nabla I^e = \frac{\sigma^e T_e - I^e}{\lambda^e},$$
$$\boldsymbol{q}_e = \int_{4\pi} \boldsymbol{n}\, I^e \, \mathrm{d}\boldsymbol{n},$$

- Lagrangian frame, 2T single fluid, IB laser deposition, SESAME
- Nonlocal radiation and electron transport
- Inherent coupling of nonlocal transport and energy equations via $I = a(\boldsymbol{x}, \boldsymbol{n})\, T_e + b(\boldsymbol{x}, \boldsymbol{n})$, which leads to a temperature dependence of energy fluxes $\boldsymbol{q}_e + \boldsymbol{q}_R = \mathbf{A}\, T_e + \boldsymbol{b}$